



Directional rock mass rating (DRMR) for anisotropic rock mass characterization

Vahid Maazallahi¹ · Abbas Majdi¹

Received: 11 October 2019 / Accepted: 10 February 2021 / Published online: 1 April 2021
© Springer-Verlag GmbH Germany, part of Springer Nature 2021

Abstract

Rock mass classification systems are used to categorize and estimate the role of the most significant parameters influencing rock mass behavior to represent an equivalent continuum. Generally, in these methods, the impact of the related parameters is considered uniform in all directions. Hence, these systems describe the rock mass as an isotropic medium. In some cases, in particular, for layered strata and systematically fractured rocks, the assumption of isotropic behavior may not provide realistic results. Hence, in this paper, to characterize the rock mass anisotropy, a directional rock mass rating (DRMR) has been proposed based on the well-known rock mass rating (RMR). So, DRMR provides a three-dimensional rock mass rating, quantitatively. By means of statistical distribution of DRMR, a classification for the degree of anisotropy of rock mass has been proposed. Furthermore, a criterion to identify the prominent rock mass, isotropic/transversely isotropic/anisotropic situation, is presented. Then the stereonet has been used to demonstrate an all-round graphical representation of DRMR. This with DRMR provides an illustrative insight into the actual rock mass condition and can assist to select the appropriate method for further analysis. Also, the method can be used as a basis to develop practical solutions for many rock engineering issues, such as characterizing the mechanical parameters of rock mass as an anisotropic equivalent continuum, selective directional rock mass improvement, and proper selection of rock tunnel and rock cavern alignments. Finally, the results of some practical applications of the method, based on field data, are presented.

Keywords DRMR · Rock mass characterization · RMR · Degree of anisotropy

Abbreviations

A	Constant (Donath, 1961 equation)	DR1	Directional Rating of uniaxial compressive strength
AI	Anisotropy index based on DRMR	DR2	Directional Rating of fracture frequency
AI _m	Anisotropy index of average DRMR	DR3	Directional Rating of discontinuities conditions
B	Constant (Tziallas et al. 2013 equation)	DR4	Directional Rating of groundwater conditions
CR ^k	Condition Rating of k th discontinuity	DRMR	Directional Rock Mass Rating
CR ^k _i	Condition Rating of k th discontinuity along i-direction	DRMR ^{ave}	Average value of DRMR
D	Constant (Donath, 1961 equation)	DRMR ^{max}	Maximum value of DRMR
Dip	Dip angle of discontinuity set	DRMR ^{min}	Minimum value of DRMR
Dip ^{ip}	Dip angle of isotropic plane of intact rock	GSI	Geological Strength Index
DipDir	Dip direction of discontinuity set	P _{wl}	Percentage of soft layers thickness in heterogeneous rock strata
DipDir ^{ip}	Dip direction of isotropic plane of intact rock	R _c	Anisotropy index of intact rock
		R _{cm}	Anisotropy index of rock mass
		RMR	Rock Mass Rating
		RQD	Rock Quality Designation
		RQD _i	Rock Quality Designation along i-direction
		S _i	Average spacing of discontinuities along i-direction
		UCS _i	UCS of anisotropic intact rock along i-direction

✉ Abbas Majdi
amajdi@ut.ac.ir

¹ School of Mining Engineering, College of Engineering, University of Tehran, Tehran 1439957131, Iran

X, Y, Z	Global Cartesian axes
a	Constant (Hoek-Brown failure criterion)
c_i	Cohesion of intact rock
c_j	Cohesion of discontinuities
i	Arbitrary direction to calculate DRMR
k	Discontinuity number ($k = 1$ to n)
n	Number of discontinuity sets
s	Constant (Hoek-Brown failure criterion)
\bar{s}^k	Average spacing of k^{th} discontinuity set
\mathbf{u}^{ip}	Unit normal vector of isotropic plane of intact rock
$u_x^{ip}, u_y^{ip}, u_z^{ip}$	Components of \mathbf{u}^{ip} in global Cartesian coordinates
\mathbf{u}^k	Unit normal vector of k^{th} discontinuity
u_x^k, u_y^k, u_z^k	Components of \mathbf{u}^k in global Cartesian coordinates
\mathbf{v}	Unit vector of arbitrary direction i
v_x, v_y, v_z	Components of \mathbf{v} in global Cartesian coordinates
v_x, v_y, v_z	Components of \mathbf{v} in local Cartesian coordinates
x, y, z	Local Cartesian axes
β	Angle between loading direction and isotropic plane/discontinuity
β_m	Angle β at which the UCS of anisotropic rock is minimum
θ_i^k	Angle between normal vector of k^{th} discontinuity and i -direction
θ_i^{IP}	Angle between normal vector of isotropic plane and i -direction
λ_i	Cumulative linear frequency of discontinuities along i -direction
λ^k	linear frequency of k^{th} discontinuity set
λ_i^k	Linear frequency of k^{th} discontinuity set along i -direction
ρ	Trend of arbitrary direction
ρ_d	Trend of pole of discontinuity
ρ_{ip}	Trend of pole of isotropic plane of intact rock
σ_{1f}	Major principal stress at failure
σ_3	Confining minor principal stress
σ_{ci}	Uniaxial compressive strength of intact rock
σ_{ci}^{max}	Maximum uniaxial compressive strength of intact rock
σ_{ci}^{min}	Minimum uniaxial compressive strength of intact rock
σ_{cm}	Equivalent uniaxial compressive strength of jointed rock mass
σ_{cm}^{max}	Maximum uniaxial compressive strength of rock mass
σ_{cm}^{min}	Minimum uniaxial compressive strength of rock mass
σ_{ci}^h	Equivalent strength of intact rock in heterogeneous medium
σ_{ci}^S	Uniaxial compressive strength of stronger rock layers in heterogeneous medium

$\sigma_{c\beta}$	UCS of anisotropic rock at orientation angle β
φ_i	Internal friction angle of intact rock
φ_j	Internal friction angle of discontinuities
ψ	Plunge of arbitrary direction
ψ_d	Plunge of the pole of discontinuity
ψ_{ip}	Plunge of pole of isotropic plane of intact rock
ω	Rotation angle of the local coordinates

Introduction

Engineering rock mass classification systems are basically used to provide guidelines of stability performance and to select an appropriate support for any underground spaces. The other significant application of these systems is to estimate the equivalent properties of the rock masses. Hence, the classification systems have often been used in cycle with analytical and numerical tools (Lin et al. 2013; Huan et al. 2019). In this approach, the representative parameters of the jointed rock mass are determined through empirical relations; and then, the problem is solved by employing analytical and numerical techniques available for the continuum medium.

Despite the lack of appropriate mathematical base for the creation of a characteristic model, engineering rock mass classification systems have found wide acceptance in studies of different phases of analyses and design of geomechanical structures. In these classifications, combined effects of many factors, such as properties of intact rock and discontinuities, earth stresses, and groundwater, are taken into account, depending on the type of classification. These systems are considered as a part of equivalent continuum approach to determine the equivalent parameters of the rock media. Practically speaking, in an equivalent continuum analysis, selection of a suitable model is solely based on the ease of accessibility of the required input parameters with acceptable accuracy (González et al. 2016). It is worthwhile to mention that the selected model must be capable enough to represent the realistic field, either isotropic or anisotropic geomechanical situation.

Most of the rocks exhibit some degrees of anisotropy due to the existence of structural defects such as bedding planes, foliations, fracturing, or joints (Chen et al. 1998). The rock mass anisotropy is found in systematically fractured rocks, sedimentary formations consisting of alternating layers, and metamorphic formations. According to Ramamurthy (1993), anisotropy may be due to either the intrinsic nature of the rock (e.g., foliation, schistosity, and cleavages) or the extrinsic sources (e.g., existence of fractures and/or sequences of different rock layers). So, the former cause is known as the inherent anisotropy, whereas the latter one is termed as the

induced anisotropy (Ramamurthy 1993; Heng et al. 2015). Anisotropy plays an important role in various earthwork engineering activities such as rock slope stability and the stability of underground openings (Majdi and Hassani 1989).

However, despite the wide applications of rock engineering classifications, few researchers have used them to describe the anisotropy of rock mass. The very first accessible rock classification system was given by Agricola (1556). He proposed a qualitative classification for ores and surrounding rocks. The other early known attempt to provide a method for rock mass classification was due to by Ritter (1879). However, rock load classification by Terzaghi (1946) was the pioneering classification system for the design of tunnel support. In this system, the rock mass is categorized into seven groups by a descriptive method, and the rock load on steel sets is estimated. Then after, stand-up time classification has been proposed by Lauffer (1958) and modified by Pacher et al. (1974), to estimate the stand-up time for an unsupported span of the tunnel based on the surrounding rock mass quality. One of the first attempts to provide a quantitative description of rock mass quality was by Deere et al. (1967), which was the introduction of the rock quality designation (RQD) system. Wickham et al. (1972) presented Rock Structure Rating (RSR) as the first multi-parameter system for rock mass classification. Bieniawski (1973, 1976, 1979, 1989) developed a system for accounting contributions of different factors on the final rock mass quality decision; which is known as either geomechanics classification or as the Rock Mass Rating (RMR) system. However, Barton et al. (1974) introduced rock tunneling quality index or the Q-system, shortly after. The two later systems are considered as the basis for developing many other systems for engineering rock mass classification. Then after, geological strength index (GSI) was proposed by Hoek (1994) to characterize both weak and hard rock masses. Palmström (1995) introduced the rock mass index (RMi) to estimate the uniaxial compressive strength of rock mass. Marinos and Hoek (2001) further improved the GSI system by introducing a chart for visual inspection of rock mass. Recently, rock mass quality rating (RMQR) has been introduced by Aydan et al. (2014) for estimation of geomechanical characteristics of rock masses.

Among the abovementioned systems, RMR, Q, and GSI are the widely used classifications for characterizing the rock mass and determining its equivalent strength and deformation parameters. Although RMi provides a good description of the rock mass in terms of effective parameters, however, its application is much less than those methods that were given before. The RMQR is an interesting engineering rock classification system which takes significant number of geomechanical factors into account; however, it requires more

field applications to appreciate its credibility. Older classifications such as Terzaghi (1946), Lauffer (1958), Pacher et al. (1974), RQD, and RSR nowadays form the basis for education of the application of rock engineering.

To date, various studies have proven that RMR system is an easy and reliable rock engineering classification system with relatively less expertise requirement (Sen and Sadagah 2003). Rock mass rating (RMR) was originally proposed by Bieniawski based on tunneling experiences in South Africa. He further modified the RMR in 1979 and in 1989. RMR has been used as a basis for developing many other rock mass classification systems, such as Mining Rock Mass Rating (MRMR) (Laubscher 1990), IRMR (Jakubec and Laubscher 2000), CMRI-RMR (CMRI 1987; Venkateswarlu et al. 1989), Surface Rock Classification (SRC) (Gonzalez de Vallejo 1983, 1985, 2003), slope mass rating (SMR) (Romana 1985), CSMR (Chen 1995), continuous RMR (Sen and Sadagah 2003), continuous SMR (Tomas et al. 2007), and GRMR (Khatik and Nandi 2018).

Though the existing engineering rock mass classification systems are well-established methods in rock mass characterization, the methods simplify the rock mass behavior to an isotropic condition. However, a very newly proposed method “anisotropic rock mass rating (ARMR)” has been given by Saroglou et al. (2018) which considers the anisotropic rock masses. So, the system takes the “strength anisotropy index” into account as a new rating component, and then the final rating is adjusted according to the effect of confining stress. The total rating of the method is an inverse indicator of the rock mass anisotropy. However, the application of ARMR is limited to only transversely isotropic rock masses with dominant inherent anisotropy with the presence of maximum one or two discontinuity sets.

Since all parameters of the rock mass classifications are scalar, therefore, they cannot assess rock mass anisotropy (Wu and Kulatilake 2012). Hence, in these methods, considering the anisotropy is an important step in their development and leads to a more realistic description of the rock mass. Therefore, the main objective of this study is to provide an empirical approach to describe the anisotropic characteristics of a rock mass. For this purpose, the RMR classification system has been selected as the base system. The reason for choosing this system is its wide and easy application (Sen and Sadagah 2003) and its good relation with rock mass mechanical parameters (Aksoy 2008). The later issue is of high importance for further developments of the method for characterizing the rock mass parameters as an anisotropic equivalent continuum. Hence, in this paper, a “directional rock mass rating (DRMR)” is proposed to take the aforesaid conditions into account. The basic designated solution to develop DRMR is determination of the corresponding rating parameters, directionally. DRMR is capable to characterizes the rock mass in any arbitrary direction and/or on a three-dimensionally

continuous space so that the rock mass anisotropy can be well recognized and dealt with. By this approach, the proper behavioral model of rock mass can be identified from isotropy/anisotropy point of view.

Directional rock mass rating (DRMR), methodology and development

The main objective of this paper is to develop a rock mass classification system to represent the realistic field: isotropic and anisotropic geomechanical situation, independently. To do so, RMR classification system is selected as a base, due to its satisfactory performance in dealing with rock engineering issues. Upon this, a directional rock mass rating (DRMR) is introduced hereafter. Due to well establishment of RMR for determination of equivalent parameters of jointed rocks, the same classification parameters and ratings are adopted to develop DRMR as well. Hence, the attempt is to rate the classification parameters directionally. Basically, RMR includes five classification parameters:

- Intact rock's uniaxial compressive strength (UCS)
- Rock quality designation (RQD)
- Discontinuities' spacing
- Discontinuities' conditions
- Groundwater conditions

Details of the rock mass rating system are presented in Table 1 which gives the rating for each of the parameters listed above. Summation of these ratings after adjustment for discontinuities' orientations yields the value of RMR.

After 40 years of application of RMR, Lawson and Bieniawski (2013) recommended against further use of RQD in the RMR system. Pells et al. (2017) presented the limitations to the use of RQD and concluded that it should be phased out in rock mass classification systems. Hence, in the 2013 version of RMR, the ratings of RQD and discontinuity spacing have been combined and taken into account by "fracture frequency." For improved accuracy, charts of Fig. 1 have also been proposed for continuous rating of uniaxial compressive strength and fracture frequency instead of the stepwise manner. Neither of these revisions changed the basic allocation of rating values to the RMR parameters.

To calculate DRMR, the classification parameters are required to be determined along with the desired direction(s). Since DRMR is naturally directional, hence, the rating adjustment for discontinuities' orientations is not taken into consideration. Also, the approach of using the fracture frequency instead of RQD and discontinuities' spacing is followed. For this purpose, the directional rating is defined for each of the aforementioned parameters, individually. These ratings are denoted by DR1–DR4, so that:

- DR1 is the directional rating of uniaxial compressive strength
- DR2 is the directional rating of fracture frequency
- DR3 is the directional rating of discontinuities' conditions
- DR4 is the directional rating of groundwater

Finally, DRMR is calculated by algebraic summation of these ratings. The following sections outline the determination of DR1 to DR4, respectively.

DR1—directional rating of uniaxial compressive strength

Almost all rocks, to some extent, are anisotropic in their mechanical properties (Barton and Quadros 2014). Basically, intact rocks with random grain structures (Fig. 2a) behave isotropic, while those with linear or planar grain structures (Fig. 2b) likely behave anisotropic in strength and deformability (Wittke 2014). For example, rocks such as sandstone and conglomerate indicate low strength anisotropy, while schistose rocks such as schists and shales are generally known as highly anisotropic. The anisotropy which is caused due to internal structure of intact rock is termed intrinsic anisotropy.

Accordingly, if the rocks have intrinsic strength anisotropy, it is necessary to determine their strength in anisotropic manner. To do so, the uniaxial compressive strength tests/point load tests must be carried out on the extracted samples in the desired directions. Schmidt hammer test can also be used for this purpose.

Another strength anisotropy that must be considered in directional rating of UCS is the anisotropy induced by alternation of rock layers with different strength properties whose overall behavior as a rock mass would be different along with and perpendicular to the bedding planes (Fig. 2c). In these media, the degree of anisotropy depends on two parameters: the strength difference and the thickness ratio of the alternating strong and weak layers.

According to the available references, a guideline has been designed to estimate the uniaxial compressive strength of the intact rock with reference to the anisotropy condition of rock media (Table 2). Based on this guideline, for the case of linear/planar grain structure rocks, a set of laboratory tests must be carried out on oriented rock samples. In this case, the uniaxial compressive strength of intact rock can be well described by the following equation, which was initially proposed by Jaeger (1960) and later modified by Donath (1961):

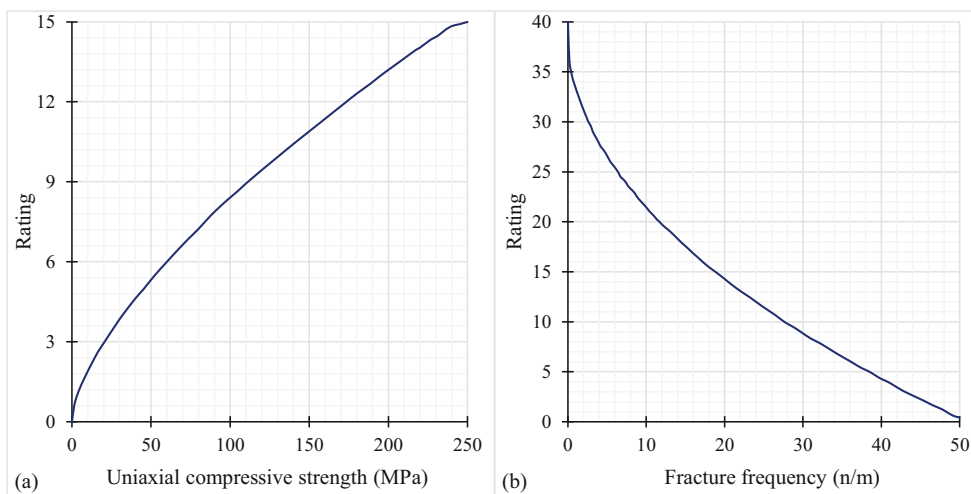
$$\sigma_{c\beta} = A - D[\cos 2(\beta_m - \beta)] \quad (1)$$

where β is the angle between loading direction and isotropic planes of the intact rock, β_m is the angle at which the

Table 1 Rock mass rating system—classification parameters and their ratings (after Bieniawski 1989)

Parameter	Range of values					
1 Strength of intact rock material	Point load strength index (MPa)	>10	4–10	2–4	1–2	For this low-range uniaxial compressive test is preferred
Rating	Uniaxial comp. strength (MPa)	>250	100–250	50–100	25–50	5–25 1–5 <1
2 Drill core quality RQD	Rating	15	12	7	4	2 1 0
Rating	90–100%	75–90%	50–75%	25–50%	25–50%	< 25%
3 Spacing of discontinuities	Rating	20	17	13	8	3
Rating	>2m	0.6–2 m	200–600 mm	60–200 mm	60–200 mm	< 60 mm
4 Condition of discontinuities (Also see Table 3)	Rating	20	15	10	8	5
Rating	Very rough surfaces	Slightly rough surfaces	Slightly rough surfaces	Slightly rough surfaces	Slackensided surfaces	Soft gouge >5 mm thick
Rating	Not continuous	Separation <1 mm	Separation <1 mm	Separation <1 mm	Gouge <5 mm thick	Separation >5 mm
Rating	No separation	Slightly weathered walls	Highly weathered walls	Highly weathered walls	Separation 1–5 mm	Continuous
Rating	Unweathered walls	Unweathered walls	Unweathered walls	Unweathered walls	Continuous	Continuous
5 Groundwater	Rating	30	25	20	10	0
Rating	Inflow per 10 m tunnel length (l/m)	None	< 10	10–25	25–125	> 125
Rating	(Joint water press)/ (major principal stress)	0	< 0.1	0.1–0.2	0.2–0.5	> 0.5
Rating	General conditions	Completely dry	Damp	Wet	Dripping	Flowing
Rating	General conditions	15	10	7	4	0
Rating adjustment for joint orientations:	Rating	Very favorable	Favorable	Fair	Unfavorable	Very unfavorable
Strike and dip orientation of joints	Rating	0	-2	-5	-10	-12
Tunnels	Rating	0	-2	-7	-15	-25
Foundations	Rating	0	-5	-25	-50	-60
Slopes	Rating	0	-5	-25	-50	-60

Fig. 1 Rating charts for RMR parameters; **a** uniaxial compressive strength of intact rock, **b** fracture frequency (Lowson and Bieniawski 2013)



uniaxial compressive strength is the minimum (usually between 30 and 45°), and A and D are constants. The constants A and D can be determined, if the uniaxial compressive strength is known at least at three different loading angles, preferably at $\beta = 0^\circ, 30^\circ,$ and 90° . In other words, to obtain A and D , for any specific cases, at least three uniaxial compression tests must be conducted on rock samples with the aforementioned orientations. The results of laboratory tests on some anisotropic rock samples and their corresponding fitted strength curve are depicted in Fig. 3.

For DR1 determination, the uniaxial compressive strength must be estimated for the desired direction(s). For this purpose, UCS_i is introduced which represents the uniaxial compressive strength along with an arbitrary i -direction within the 3D space. To calculate UCS_i based on Eq. 1, the angle β between the arbitrary i -direction and the isotropic planes of the intact rock must be obtained. Instead of β , its complementary angle, θ , can be obtained by using vector analysis. Hence, the arbitrary direction of rating can be defined by a unit vector

\mathbf{v} , whose components in global Cartesian coordinate system, $v_x, v_y,$ and v_z , are given as follows (Fig. 4):

$$v_x = \sin \rho \cos \psi \tag{2}$$

$$v_y = \cos \rho \cos \psi \tag{3}$$

$$v_z = \sin \psi \tag{4}$$

where ρ and ψ are the trend and the plunge of the arbitrary direction, respectively.

For the aforementioned case of rocks with linear/planar grain structure, the isotropic plane of intact rock can also be described by its normal vector \mathbf{u}^{ip} , whose components in global Cartesian coordinate system, $u_x^{ip}, u_y^{ip},$ and u_z^{ip} , are given as follows:

$$u_x^{ip} = \sin \rho_{ip} \cos \psi_{ip} \tag{5}$$

$$u_y^{ip} = \cos \rho_{ip} \cos \psi_{ip} \tag{6}$$

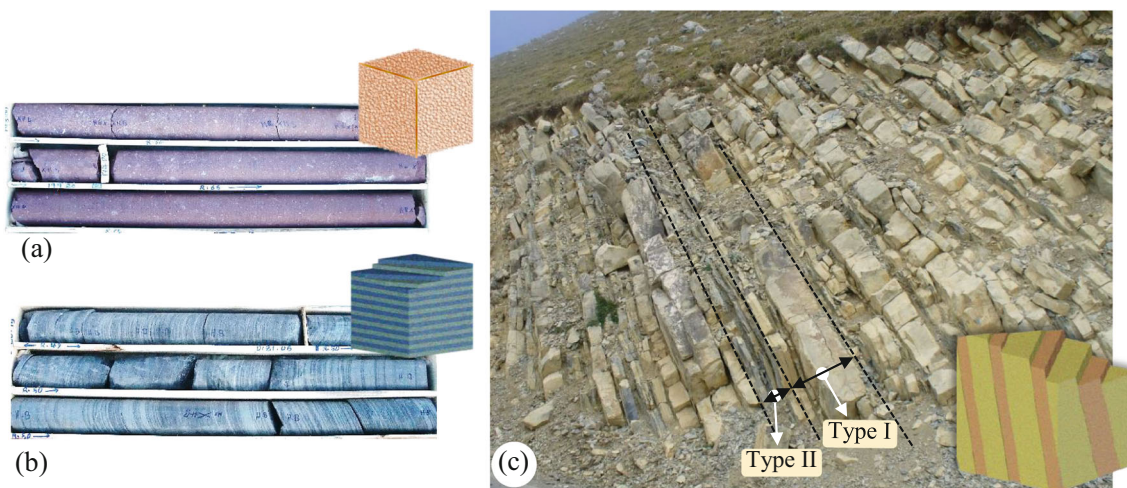


Fig. 2 **a** A random grain structure rock, **b** a planar grain structure rock (pictures of rock cores taken from Kerman water conveyance tunnel under construction, Kerman, Iran), **c** rock mass anisotropy due to alternating rock layers; an actual case from Masal, Gilan, Iran

Table 2 A guideline for determination of the uniaxial compressive strength of intact rock with reference to the anisotropy condition of rock media

Rock media	Example	Isotropy condition	Determination of UCS of intact rock	
Homogeneous	Random grain structure Linear/planar grain structure	Massive igneous and sedimentary rocks Schistose/foliated/bedded metamorphic and sedimentary rocks	Isotropic Transversely isotropic/-anisotropic	Uniaxial compression/point load test Variations of anisotropic strength can be obtained by conducting a set of uniaxial compression/point load tests on oriented rock samples with regard to the direction of isotropic planes. Some typical equations are available to describe these variations: General equation by Jaeger (1960) that modified by Donath (1961): $\sigma_{c\beta} = A - D[\cos 2(\beta_m - \beta)]$ Also see Donath (1964) and Ajalloeian and Lashkaripour (2000) equations for mudstones, Singh et al. (2001) for schistose rocks, Garagon and Can (2010) equations for sandstones
Heterogeneous	Alternation of different rock layers	Sedimentary sequences consisting of strong and weak rock	Transversely isotropic/-anisotropic	$\sigma_{ci}^h = \sigma_{ci}^S \cdot e^{-B \cdot P_{vol}}$ based on Tziailas et al. (2013). Determination of UCS_i using GSI according to Marinou and Hoek (2001), Hoek et al. (2005), Marinou (2010)

$$u_z^{ip} = \sin \psi_{ip} \tag{7}$$

where ρ_{ip} and ψ_{ip} are the trend and the plunge of the pole of the isotropic plane, respectively, and are related to dip direction and dip of the isotropic plane ($DipDir^{ip}/Dip^{ip}$) by the following relations:

$$\rho_{ip} = \begin{cases} DipDir^{ip} + 180^\circ & (for\ DipDir^{ip} < 180^\circ) \\ DipDir^{ip} - 180^\circ & (for\ DipDir^{ip} \geq 180^\circ) \end{cases} \tag{8}$$

$$\psi_{ip} = 90^\circ - Dip^{ip} \tag{9}$$

The angle θ_i^{ip} between the normal to the isotropic plane and the arbitrary i -direction can be calculated as follows:

$$\cos \theta_i^{ip} = u_x^{ip} \cdot v_x + u_y^{ip} \cdot v_y + u_z^{ip} \cdot v_z \tag{10}$$

Thus, by substituting Eqs. 2, 3, 4, 5, 6, 7, 8, and 9 into Eq. 10 and considering that θ_i^{ip} is in the range of 0–90°, the following

relation is obtained to calculate θ_i^{ip} for the prescribed i -direction:

$$\theta_i^{ip} = \cos^{-1} |\cos(Dip^{ip}) \sin \psi - \sin(Dip^{ip}) \cos \psi \cos(DipDir^{ip} - \rho)| \tag{11}$$

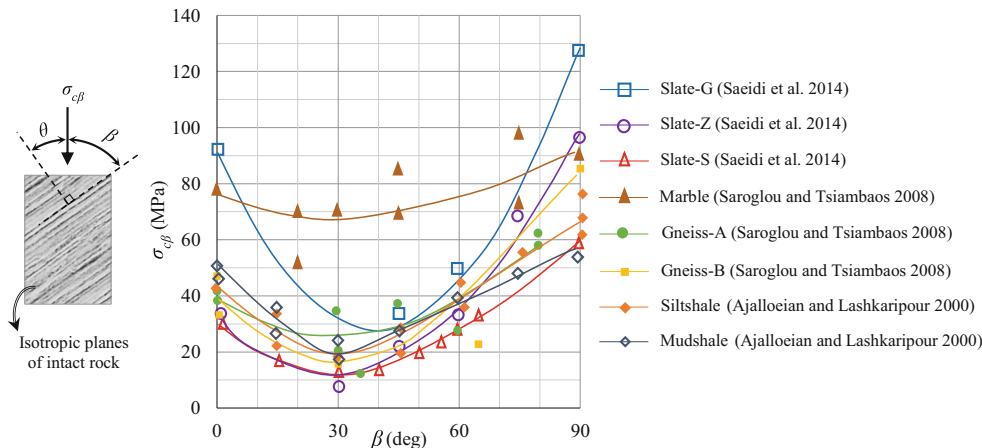
Then, bearing in mind that θ_i^{ip} and β are complementary angles, UCS_i can be calculated for the prescribed i -direction by substituting $\beta = 90 - \theta_i^{ip}$ into Eq. 1, which leads to the following relation:

$$UCS_i = A + D [\cos 2(\beta_m + \theta_i^{ip})] \tag{12}$$

Consequently, once the directional intact rock strength is determined, then its corresponding rating, $DR1_i$, could be calculated by the following relation which is the mathematical expression of graph of Fig. 1a:

$$DR1_i = 0.45(UCS_i)^{0.636} \tag{13}$$

Fig. 3 Uniaxial compressive strength of some intact rocks with linear/planar grain structure; laboratory data and the fitted curves based on Eq. 1 (After Ajalloeian and Lashkaripour 2000; Saroglou and Tsiambaos 2008; Saeidi et al. 2014)



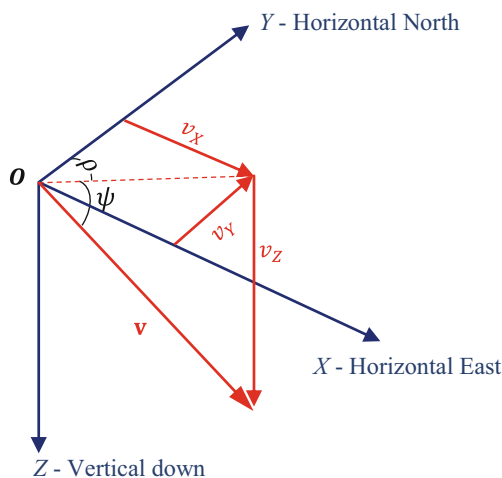


Fig. 4 Definition of an arbitrary direction for rating as a unit vector and its components in global Cartesian coordinates

DR2—directional rating of fracture frequency

Following the RMR₁₃ approach, fracture frequency, which is the number of discontinuities per unit length, is used to take the combined rating of RQD and discontinuities’ spacing into account. Fracture frequency is a function of mapping direction and indeed the angle between scan line and discontinuity planes (Zhang 2016). Figure 5 presents this relationship for a single joint set. As shown in Fig. 5, fracture frequency as the inverse of joint spacing is the maximum and the minimum in the directions perpendicular to and parallel with the joint set, respectively. This difference, certainly, leads to the different behaviors of rock mass along with various directions (i.e., anisotropy). This is more obvious when the strength parameters of the discontinuities are considerably different with those of intact rocks. Therefore, determination of this parameter for the presumed directions is among the most important factors in DRMR characterization.

The geological mapping commonly includes positioning, recording, statistical analysis, and graphical illustration of geological phenomena and structures on topographical maps or geological sections. Spatial situation of discontinuities is described by their orientation which is recorded often in the dip direction and dip format (*DipDir/Dip*). To illustrate these measurements, a

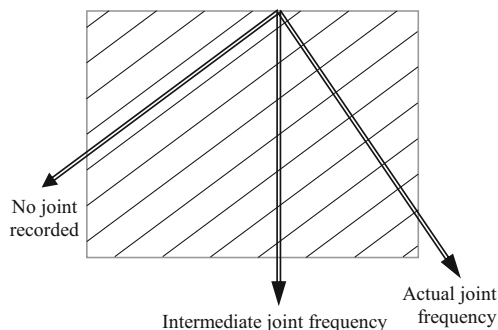


Fig. 5 Dependency of recorded fracture frequency to the drill hole orientation

stereonet with a spherical projection system is used. The bias on the recorded data (dip direction, dip, and spacing) due to the alignment of sampling line must be corrected by means procedures outlined in geological mapping references.

To calculate the discontinuities’ frequency along an arbitrary direction, the same vector analysis can be implemented as described in the section “DR1—directional rating of uniaxial compressive strength.” Hence, the prescribed direction of rating as unit vector **v** is used. Similarly, any discontinuity can also be described by its normal vector **u^k**, where *k* superscript represents the discontinuity number. The components of **u^k** in global Cartesian coordinate system, *u^k_X*, *u^k_Y*, and *u^k_Z*, can be obtained by replacing the superscript *ip* with *k* in Eqs. 5, 6, 7, 8, and 9.

Hence, the angle between the normal to the *kth* discontinuity and the arbitrary *i*-direction, θ_i^k , is as follows:

$$\theta_i^k = \cos^{-1} |\cos(Dip^k) \sin \psi - \sin(Dip^k) \cos \psi \cos(DipDir^k - \rho)| \tag{14}$$

On the other hand, the linear frequency of *kth* discontinuity set, λ^k , is:

$$\lambda^k = \frac{1}{\bar{s}^k} \tag{15}$$

where \bar{s}^k is the average spacing of *kth* discontinuity set. Hence, the directional linear frequency of *kth* discontinuity set along the arbitrary *i*-direction, λ_i^k , can be calculated as follows:

$$\lambda_i^k = \lambda^k |\cos \theta_i^k| \tag{16}$$

Then, the cumulative directional linear frequency for *n* discontinuity sets along the arbitrary *i*-direction, λ_i , could be computed:

$$\lambda_i = \sum_{k=1}^n \lambda_i^k \tag{17}$$

or in the complete form:

$$\lambda_i = \sum_{k=1}^n \left[\frac{1}{\bar{s}^k} |\cos(Dip^k) \sin \psi - \sin(Dip^k) \cos \psi \cos(DipDir^k - \rho)| \right] \tag{18}$$

Finally, DR2_{*i*} can be determined by the following equation which is the mathematical expression of graph of Fig 1b:

$$DR2_i = 40 - 5.7(\lambda_i)^{0.5} \tag{19}$$

DR3—directional rating of conditions of discontinuities

There are five factors that are involved in determining the rating of discontinuities’ conditions: persistence, aperture, roughness, infilling, and weathering (Table 3). The sum of these factors provides a quantitative description of the quality

Table 3 Rock mass rating system—guidelines for classification of discontinuity condition (after Bieniawski 1989)

Parameter	Range of values and their corresponding rating				
Discontinuity length (persistence)	< 1 m	1–3m	3–10 m	10–20 m	>20 m
Rating	6	4	2	1	0
Separation (aperture)	None	<0.1 mm	0.1–1.0 mm	1–5 mm	> 5mm
Rating	6	5	4	1	0
Roughness	Very rough	Rough	Slightly rough	Smooth	Slickensided
Rating	6	5	3	1	0
Infilling (gouge)	None	Hard filling <5mm	Hard filling >5mm	Soft filling <5mm	Soft filling >5mm
Rating	6	4	2	2	0
Weathering	Unweathered	Slightly weathered	Moderately weathered	Highly weathered	Decomposed
Ratings	6	5	3	1	0

Note: Some conditions are mutually exclusive. For example, if infilling is present, the roughness of the surface will be overshadowed by the influence of the gouge. In such cases use Table 1 directly.

of the discontinuities. It is obvious that each of these factors has an effect on the strength of the discontinuities and thus the rock mass strength. Therefore, a procedure that is capable to describe these effects can be used as a basis for determination of directional rating of discontinuities conditions. Any discontinuity can reduce the rock mass strength properties including compressive strength and deformation modulus. Since the compressive strength is considered as one of the main pillars of some classification systems, especially RMR, therefore, the effect of discontinuities on this parameter is taken as the basis for the development of DRMR and directional rating of discontinuities' conditions. For this purpose, the theory of "single plane of weakness," proposed by Jaeger (1960), is used. In this theory, the modeled rock mass is cut by a single discontinuity set (Fig. 6a). Then, the equivalent continuum strength of the rock mass is determined by analytical solution. Various models have been proposed based on this theory. Jaeger (1960) and Jaeger and Cook (1979) presented a model for jointed rock mass under axisymmetric loading condition. The latter authors described the strength of both the intact rock and the discontinuities by Mohr-Coulomb criterion. Based on

this model, the major principal stress causes shear failure, σ_{1f} along the discontinuity or through the intact rock which can be computed by Eq. 20 and Eq. 21, respectively.

$$\sigma_{1f} = \sigma_3 + \frac{2(c_j + \sigma_3 \tan \varphi_j)}{\sin 2\beta (1 - \tan \varphi_j \tan \beta)} \tag{20}$$

$$\sigma_{1f} = 2c_i \tan\left(\frac{\pi}{4} + \frac{\varphi_i}{2}\right) + \sigma_3 \tan^2\left(\frac{\pi}{4} + \frac{\varphi_i}{2}\right) \tag{21}$$

where c_i and φ_i are the cohesion and internal friction angle of the intact rock, respectively, and c_j and φ_j are the cohesion and internal friction angle of the discontinuities, respectively.

The equivalent uniaxial compressive strength of jointed rock mass, σ_{cm} , is equal to the minimum of values obtained by substituting $\sigma_3 = 0$ in Eqs. 20 and 21, hence:

$$\sigma_{cm} = \min \left\{ \begin{array}{l} \frac{2c_j}{\sin 2\beta (1 - \tan \varphi_j \tan \beta)} \\ 2c_i \tan\left(\frac{\pi}{4} + \frac{\varphi_i}{2}\right) \end{array} \right. \tag{22}$$

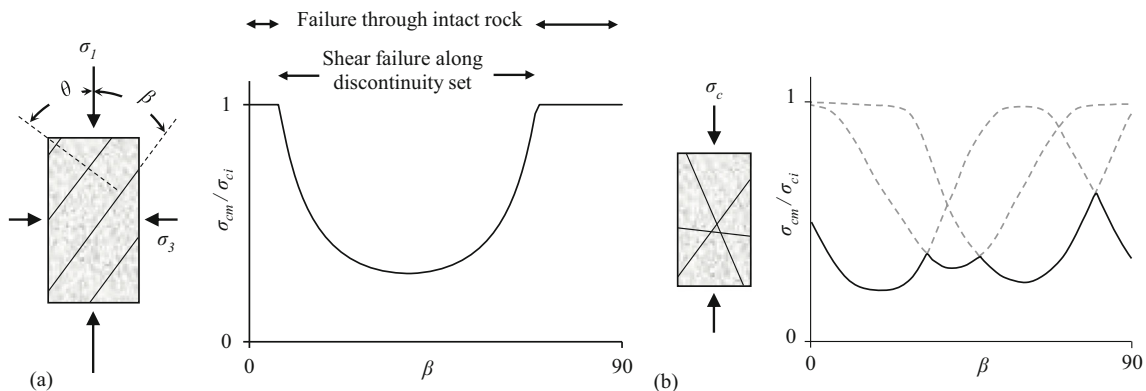


Fig. 6 Theory of single plane of weakness: jointed rock mass model and variations of σ_{cm}/σ_{ci} versus β for a rock mass containing **a** one discontinuity set, **b** more than one discontinuity set (Jaeger 1960; Jaeger and Cook 1979)

By this formulation, the maximum equivalent uniaxial compressive strength is generally found when the loading direction is nearly perpendicular to or parallel with the discontinuity plane, while the minimum strength is obtained when the angle β between the loading direction and the discontinuity plane is at 30–60° (Zhang 2017) (Fig. 6a). However, rock mass generally contains more than one discontinuity set. For the case of a rock mass with several discontinuity sets, the equivalent strength of the rock mass is obtained by considering the effects of all discontinuity sets, simultaneously (Jaeger and Cook 1979; Hudson and Harrison 2000). So, at any angle β , the smallest strength of the existing discontinuities will be chosen as the resultant strength of the rock mass (Fig. 6b).

The basic idea used for the determination of directional rating of discontinuities' conditions is to follow the same concept as is provided by the aforementioned theory of single plane of weakness. So, first, the directional condition rating of each discontinuity set is determined. Then, at any angle β , the smallest directional condition rating of existing discontinuities will be chosen as the resultant DR4.

With this approach, the directional condition rating of any discontinuity follows the same trend of variation of strength as illustrated in Fig. 6a. Based on this figure, two different ratings' trend can be distinguished with regard to β :

- For the ranges of β , when the equivalent strength of a rock mass is equal to the strength of intact rock, i.e., $\sigma_{cm}/\sigma_{ci} = 1$, then the maximum rating of 30 is assigned for.
- For the ranges of β , when the equivalent strength of rock mass exhibits a parabolic variation, then a rating of less than 30 is assigned for.

At the later ranges of β , the aforementioned parabolic trend is controlled by the strength properties of discontinuity set. The strength parameters of discontinuities can vary in a wide range; from close to intact rock parameters for very good quality joints to negligible values for very weak ones. Figure 7 illustrates the effect of variation of the strength parameters of discontinuity set on the resultant equivalent strength of the rock mass. It can be seen from this figure that, by decreasing the strength of the discontinuity set, the range of angles where shear failure occurs on the discontinuity plane expands, while the ultimate strength within this range is reduced. Hence, such a model that represents the simultaneous effects of discontinuity set orientation and its strength parameters could be a good basis of obtaining a solution for directional rating of discontinuity condition.

The effect of discontinuity set orientation can be quantified by using the angle β or its complementary angle, θ (Fig. 6a). The effect of strength properties of discontinuity set can be simulated by its condition rating, CR^k , which is determined using Table 3, and considering the role of all 5 factors. For this purpose, a direct linear relationship has been considered between the strength parameters of the discontinuity set and its condition rating. So, the rating of 30 describes a discontinuity whose strength parameters are very close to the intact rocks', while the lower boundary of this rating represents a highly low strength discontinuity. Accordingly, by applying various values of strength parameters and using multivariate regression techniques, a relationship is obtained to determine the directional rating of discontinuity conditions. Consequently, condition rating of k^{th} discontinuity along any arbitrary direction i is termed as CR_i^k and can be computed as follows:

$$CR_i^k = \begin{cases} 30 \\ 0.96 CR^k \left[\cos \left(2\theta_i^k - 90 \left(1 + \frac{CR^k}{60} \right) \right) \right]^{-(0.07 CR^k + 1)} \\ 30 \end{cases}$$

$$\begin{aligned} &\theta_i^k \leq 2.2 CR^k \\ &2.2 CR^k < \theta_i^k < 90 - 0.7 CR^k \\ &90 - 0.7 CR^k \leq \theta_i^k \end{aligned} \tag{23}$$

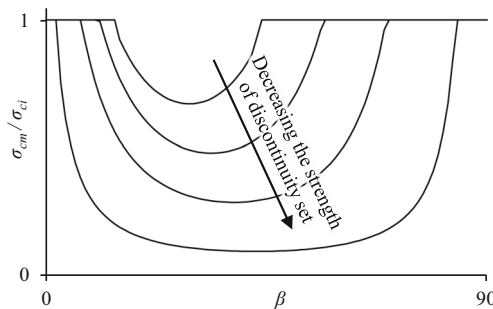


Fig. 7 Effect of variation of discontinuity strength on equivalent strength of rock mass

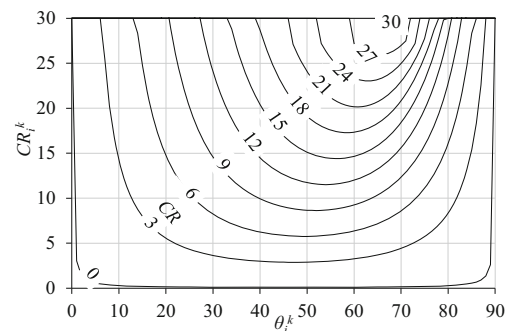


Fig. 8 Determination of directional condition rating of k^{th} discontinuity, CR_i^k , based on its condition rating CR^k and the angle θ_i^k with arbitrary direction i

in which θ_i^k is in the range of 0–90° and can be obtained by using Eq. 14.

With this approach, the directional condition rating of any given discontinuity, CR_i^k , varies from CR^k to the maximum value of 30, depending on its orientation with regard to the arbitrary direction. The representation of Eq. 23 is depicted in Fig. 8. Finally, for a rock mass containing n discontinuity sets, the directional rating of discontinuities conditions at any arbitrary direction i , $DR4_i$, can be determined using the following relation:

$$DR4_i = \min\left(CR_i^k \Big|_{k=1-n}\right) \quad (24)$$

It is worth noting that some factors of discontinuity conditions (especially the surface roughness) may exhibit an inherent anisotropy. However, in actual field applications, often this anisotropy can't be well characterized. Basically, the rating of discontinuity conditions (CR^k) must be determined by considering the combined effect of all 5 incorporated factors, i.e., persistence, aperture, roughness, infilling, and weathering. Though some studies have shown some degrees of anisotropy in the joint roughness, the interaction between this factor and the other mentioned ones is the more important issue for determination of CR^k . As it is noted in Table 3, "Some conditions are mutually exclusive. For example, if infilling is present, the roughness of the surface will be overshadowed by the influence of the gouge." Also, the aperture can have the same impact; an open aperture diminishes the effect of roughness. Consequently, here the emphasis was on the proper evaluation of conditions of each discontinuity rather than developing a complicated manner for taking the possible directional dependency of roughness into account, which in turn could bring difficulties to applicability of the method.

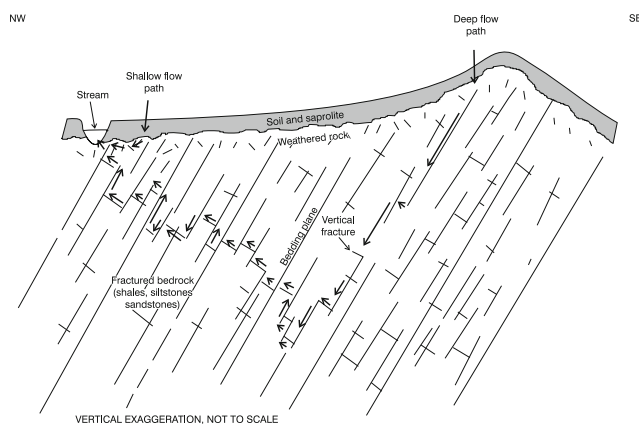


Fig. 9 A conceptual example of a groundwater flow system in a fractured sedimentary rock formation with sloping layers (Senior and Goode 1999)

DR4—directional rating of groundwater

To develop the directional rating of groundwater, it is necessary to recognize the flow mechanism within rock mass and its controlling factors. To investigate the groundwater flow in a particular area, the hydraulic conductivity or the coefficient of permeability of the medium can be evaluated. In rock media, the permeability characteristics of intact rock and rock mass are quite different. The texture of intact rock is generally composed of well-cemented mineral grains and contains some fine pores. However, these pores are generally not interconnected, which in turn leads to very low permeability of the intact rock. Due to the presence of discontinuities, the permeability of the rock mass is significantly different from the permeability of the intact rock. In most rock formations, the permeability of the matrix is low compared to the fractures' permeability. Therefore, the hydraulic behavior of rock mass is mainly under the control of fractures and their characteristics (Javadi et al. 2010). A conceptual model of the groundwater system in a fractured sedimentary rock formation is shown in Fig. 9. In this system, the groundwater flow is developed primarily along the bedding planes. Besides, although fractures perpendicular to the beddings do not cut them extensively, they can cause local water flow or leak routes between the layers (Senior and Goode 1999). This illustration indicates the governing role of discontinuities on groundwater flow, clearly.

The difference between negligible hydraulic conductivities of intact rock relative to discontinuities is used as the basis for development of the directional rating of groundwater. In this way, the directional rating of groundwater in the directions parallel to discontinuity planes is determined according to the actual flow condition of the corresponding discontinuity. For this purpose, k^{th} joint water condition, JWC^k , has to be rated from Table 1 based on its general flow condition or the ratio of its water pressure to the major principal stress. To determine JWC^k during the geological mapping, characteristics of each discontinuity set which can affect its flow behavior have to be taken into account. Characteristics such as persistence, aperture, roughness, type, and thickness of infilling could affect the permeability and thus the flow behavior of a discontinuity. Continuous persistence and wide aperture of a discontinuity naturally increase its permeability. The lower the surface roughness, the greater the hydraulic conductivity. The presence of infillings such as clay can result to a low-permeable or even an impermeable discontinuity. Hard infillings that are well interlocked to the discontinuity walls can also lead to a low hydraulic conductivity. A discontinuity without any infilling can be permeable, although tightness and interlocking of its walls can significantly reduce its permeability (Öge 2017). Anyway, joint water condition (JWC^k)

of all existing discontinuities has to be carefully evaluated during the geological mapping by taking into account the abovementioned mutual effects.

According to the above explanations, the JWC^k rating determined for each discontinuity will be assigned only to the directions that are placed on its plane. In this regard, a 10° tolerance is considered on both sides of

any discontinuity plane in order to account for possible variations of its planarity and the uncertainty of measured orientation data. In other directions, the maximum rating (i.e., 15, corresponding to dry conditions) will be assigned. Thus, based on the angle θ_i^k between the normal to the k^{th} discontinuity and the arbitrary i -direction, calculated earlier by Eq. 14, directional rating of water

Table 4 Summary of procedure to calculate DRMR along an arbitrary direction

Rating direction	Define the arbitrary direction of rating, i , in terms of its trend/plunge (ρ/ψ)					
Intact rock characteristics	Random grain structure	Isotropic UCS - determined by usual compression/point load tests				
	Rock structure	Conduct at least 3 uniaxial compression tests on oriented rock specimens; preferably at $\beta=0^\circ, 30^\circ$ and 90° . Then obtain the constants A and D and β_m by fitting a curve in the form of $\sigma_{c\beta} = A - D[\cos 2(\beta_m - \beta)]$ to the laboratory data. Take the orientation of isotropic planes of intact rock ($Dip^{ip}/DipDir^{ip}$) from geological mapping data. Calculate the uniaxial compressive strength along the arbitrary i -direction:				
		Linear/planar grain structure	EQ.1: $UCS_i = A + D[\cos 2(\beta_m + \theta_i^{ip})]$ in which: EQ.2: $\theta_i^{ip} = \cos^{-1} \cos(Dip^{ip}) \sin \psi - \sin(Dip^{ip}) \cos \psi \cos(DipDir^{ip} - \rho) $			
DR1 _i	EQ.3: $DR1_i = 0.45(UCS_i)^{0.636}$					
Fracture frequency	For n discontinuity sets: Take the orientation ($Dip^k/DipDir^k$) and spacing (\bar{s}^k) of each discontinuity set from geological mapping data. Calculate the cumulative directional linear frequency of discontinuities along the arbitrary i -direction:					
	EQ.4: $\lambda_i = \sum_{k=1}^n \left[\frac{1}{\bar{s}^k} \cos(Dip^k) \sin \psi - \sin(Dip^k) \cos \psi \cos(DipDir^k - \rho) \right]$					
DR2 _i	EQ.5: $DR2_i = 40 - 5.7(\lambda_i)^{0.5}$					
Discontinuities characteristics	For n discontinuity sets: Determine the condition rating of each discontinuity set, CR^k :					
	Condition of k^{th} discontinuity set (Also see Table 3)	Very rough surfaces Not continuous No separation Unweathered walls	Slightly rough surfaces Separation < 1 mm Slightly weathered walls	Slightly rough surfaces Separation < 1 mm Highly weathered walls	Slickensided surfaces or Gouge < 5 mm thick or Separation 1-5mm Continuous	Soft gouge > 5 mm thick or Separation > 5 mm Continuous
	CR^k	30	25	20	10	0
	Calculate the directional condition rating of each discontinuity set, CR_i^k : EQ.6: $CR_i^k = \begin{cases} 30 & \theta_i^k \leq 2.2 CR^k \\ 0.96 CR^k \left[\cos \left(2\theta_i^k - 90 \left(1 + \frac{CR^k}{60} \right) \right) \right]^{-(0.07 CR^k + 1)} & 2.2 CR^k < \theta_i^k < 90 - 0.7 CR^k \\ 30 & 90 - 0.7 CR^k \leq \theta_i^k \end{cases}$					
in which: EQ.7: $\theta_i^k = \cos^{-1} \cos(Dip^k) \sin \psi - \sin(Dip^k) \cos \psi \cos(DipDir^k - \rho) $						
DR3 _i	EQ.8: $DR3_i = \min(CR_i^k _{k=1-n})$					
Ground water	For n discontinuity sets: Determine the joint water condition of each discontinuity set, JWC^k :					
	(k^{th} Joint water press)/(Major principal stress)	0	< 0.1	0.1 - 0.2	0.2 - 0.5	> 0.5
	General conditions of k^{th} joint set	Completely dry	Damp	Wet	Dripping	Flowing
	JWC^k	15	10	7	4	0
Calculate the directional joint water condition rating of each discontinuity set, JWC_i^k :						
EQ.9: $JWC_i^k = \begin{cases} 15 & \theta_i^k < 80^\circ \\ JWC^k & 80^\circ \leq \theta_i^k \end{cases}$						
DR4 _i	EQ.10: $DR4_i = \min(JWC_i^k _{k=1-n})$					
DRMR _i = DR1 _i + DR2 _i + DR3 _i + DR4 _i						

- The classification parameters and their ratings are based on Bieniawski's RMR. However, it has been adjusted to be applicable for rating along any desired direction within 3D space, as well.

conditions of k^{th} discontinuity set, JWC_i^k , can be calculated as follows:

$$JWC_i^k = \begin{cases} 15 & \theta_i^k < 80^\circ \\ JWC^k & 80^\circ \leq \theta_i^k \end{cases} \quad (25)$$

Given the possibility of existence of different discontinuities in the media and since each of discontinuities can have different water conditions, the final directional groundwater condition rating in i -direction, $DR4_i$, can be calculated from the following equation:

$$DR4_i = \min(JWC_i^k |_{k=1-n}) \quad (26)$$

Summarized DRMR procedure

The procedure and equations to calculate DRMR are summarized and presented in Table 4 based on the explanations given in the section “DR1—directional rating of uniaxial compressive strength” to “DR4—directional rating of groundwater.” This table can be used for straightforward calculation of DRMR along any arbitrary direction within 3D space. The table guides the user for stepwise determination of DRMR. According to this table, prior to any calculations, the desired rating direction(s) must be defined by its trend and plunge. Then, based on the grain structure of intact rock, its directional uniaxial compressive strength and the corresponding directional rating, $DR1_i$, have to be determined. The next two directional ratings are dependent on the discontinuity’s characteristics. So, by means of orientations and spacing of discontinuities, the cumulative directional linear frequency and, consequently, $DR2_i$ can be calculated. Furthermore, the third directional rating, $DR3_i$, has to be determined based on conditions of discontinuity sets, as expressed in the table. The last component, i.e., $DR4_i$, can be determined based on actual water condition of joint sets and by the provided relations. Finally, DRMR can be calculated by summing up the directional ratings $DR1_i$ – $DR4_i$.

Simplified equations for rating along a local Cartesian coordinate system

In many cases, it is desired to calculate DRMR along three orthogonal directions. In these cases, rating directions can be adjusted along the axes of the global (X, Y, Z) or a local (x, y, z) Cartesian coordinate system. One of the most widely used local coordinate systems is the clockwise rotation of a horizontal plane consisting of x - and y -axes around the vertical Z -axis by ω degrees. In this case, by recalling Eqs. 11 and 18, after substitution for \mathbf{v} and \mathbf{u}^{ip} components and simplification, results are the following:

$$\theta_x^{ip} = \cos^{-1} |\sin(Dip^{ip}) \sin(DipDir^{ip}-\omega)| \quad (27)$$

$$\theta_y^{ip} = \cos^{-1} |\sin(Dip^{ip}) \cos(DipDir^{ip}-\omega)| \quad (28)$$

$$\theta_z^{ip} = \cos^{-1} |\cos(Dip^{ip})| \quad (29)$$

$$\lambda_x = \sum_{k=1}^n \left[\frac{1}{\bar{s}} |\sin(Dip^k) \sin(DipDir^k-\omega)| \right] \quad (30)$$

$$\lambda_y = \sum_{k=1}^n \left[\frac{1}{\bar{s}} |\sin(Dip^k) \cos(DipDir^k-\omega)| \right] \quad (31)$$

$$\lambda_z = \sum_{k=1}^n \left[\frac{1}{\bar{s}} |\cos(Dip^k)| \right] \quad (32)$$

It is worth noting that, in the case of $\omega=0$, the defined x - y - Z local Cartesian coordinate system reduces to the global X - Y - Z system.

Substituting the results of Eqs. 27, 28, and 29 into Eq. 12 for θ_i^{ip} determines the directional uniaxial compressive strength, UCS_i , along the local axes. Equations 30, 31, and 32 yield the directional fracture frequency along the local axes. Equations 27, 28, and 29, furthermore, can be used for calculation of θ_i^k by replacing the superscript ip with k , which then can be used to compute the condition rating of k^{th} discontinuity, CR_i^k , and also directional joint water condition, JWC_i^k , along the local axes by using Eqs. 23 and 24, respectively. Subsequently, the corresponding directional ratings, $DR1$ – $DR4$, can be determined.

DRMR illustration

By implementing the aforementioned mathematical steps, DRMR value(s) can be estimated at any arbitrary direction(s). However, the method is capable to provide a continuous all-round distribution of DRMR, as well. For this purpose, a proper net of trend-plunge values is required to cover all the probable spatial directions. An interval of 5 to 10° of trend-plunge values can provide the necessary network. Then, by calculating DRMR values for the nodes of this network, its spatial distribution will be obtained. For this purpose, calculations can be carried out simply by using a spreadsheet. The obtained spatial distribution of DRMR illustrates the actual range of variations of rock mass quality within the all-round space. Also, the values of maximum, average, and minimum DRMR can be extracted from the results of these calculations. These values are termed as $DRMR^{max}$, $DRMR^{ave}$, and $DRMR^{min}$, respectively.

To achieve the most desired representative distribution, it is suitable to use the lower hemisphere projection on a stereonet. Therefore, DRMR along with its components (if needed) can be presented in the form of contour plots on the stereonet. This type of presentation provides a quantitative all-round visualization of rock mass quality. Hence, the rock mass anisotropy and the directions of the maximum and the minimum ratings

can be well characterized. On this basis, the mechanical parameters of rock mass can be assessed within an all-round approach. This also provides a good basis for all-round evaluation of rock mass behavior and identifying the directions which exhibit high/low quality. Hence, besides anisotropic rock mass characterization, DRMR contour plots can assist in many rock engineering issues, such as determination of the most suitable alignment of underground spaces and design of directional-dependent rock mass improvement techniques. The procedure for all-round calculations and representation of DRMR, with a brief description of its applications, will be discussed in the section “An illustrated example.”

Development of an anisotropy index based on DRMR

The degree of anisotropy has been introduced as an indicator for describing the anisotropy of rocks, quantitatively. Ramamurthy (1993) defined an anisotropy index, R_c , as the ratio of the maximum uniaxial compressive strength to the minimum compressive strength of the intact rock:

$$R_c = \frac{\sigma_{ci}^{max}}{\sigma_{ci}^{min}} \tag{33}$$

Based on this index, he classified the rocks into five classes, ranging from isotropic to very highly anisotropic (Table 5).

Unlike the intact rock, there are little information about the classification of the degree of anisotropy of the rock mass. The proposed DRMR classification system has a significant potential to define an anisotropy index for the rock mass due to its rating mechanism in all-round directions. For this purpose, the compressive strength of the rock mass, σ_{cm} , is selected as the basis for development of the aforementioned index. It is obvious that there is a strong correlation between σ_{cm} and RMR (e.g., refer to: Hoek et al. 1995; Ramamurthy 1996; Sheorey 1997; Singh and Goel 1999). Since DRMR’s rating approach is similar to RMR’s one, a similar relationship can be conceived between σ_{cm} and DRMR. Hence, it can be said that DRMR’s values in different directions represent the different values of σ_{cm} . Undoubtedly, the maximum and the

Table 5 Anisotropy classification of intact rocks (Ramamurthy 1993)

Description	R_c
Isotropic	1.0–1.1
Fairly anisotropic	1.1–2.0
Moderately anisotropic	2.0–4.0
Highly anisotropic	4.0–6.0
Very highly anisotropic	> 6.0

Table 6 Anisotropy classification of the rock mass based on DRMR

Description	AI
Isotropic	0–10
Moderately anisotropic	10–25
Highly anisotropic	25–32
Very highly anisotropic	>32

minimum values of σ_{cm} are consistent with the highest and lowest DRMR ratings, respectively. Hence, substituting the maximum and the minimum values of σ_{cm} in Eq. 33 could represent a rock mass anisotropy index designated by R_{cm} , which is shown below:

$$R_{cm} = \frac{\sigma_{cm}^{max}}{\sigma_{cm}^{min}} \tag{34}$$

By using the Hoek-Brown’s strength criterion for the rock mass, σ_{cm} can be expressed as (Hoek et al. 2002):

$$\sigma_{cm} = \sigma_{ci} s^a \tag{35}$$

where s and a are constants that depend on the characteristics of the rock mass.

Hoek and Brown (1988) proposed a set of relationships between the parameters s and a , with the basic RMR. These relations for the undisturbed or interlocking rock masses are as follows:

$$s = e^{\frac{RMR-100}{9}}, \text{ and } a = 0.5 \tag{36}$$

Hence, the uniaxial compressive strength of the rock mass will be:

$$\sigma_{cm} = \sigma_c e^{\frac{RMR-100}{18}} \tag{37}$$

An acceptable approximation of the maximum and the minimum values of the uniaxial compressive strength of the rock mass can be obtained by substituting the $DRMR^{max}$ and $DRMR^{min}$ in Eq. 37, thus:

$$\sigma_{cm}^{max} \approx \sigma_{ci} e^{\frac{DRMR^{max}-100}{18}} \tag{38}$$

$$\sigma_{cm}^{min} \approx \sigma_{ci} e^{\frac{DRMR^{min}-100}{18}} \tag{39}$$

Table 7 Application of DRMR in selecting the suitable rock mass structural model

AI	AI_m	Description
≤ 10	≤ 10	Isotropic
> 10	≤ 10	Transversely isotropic
	> 10	Anisotropic

*Note that always $AI_m \leq AI$

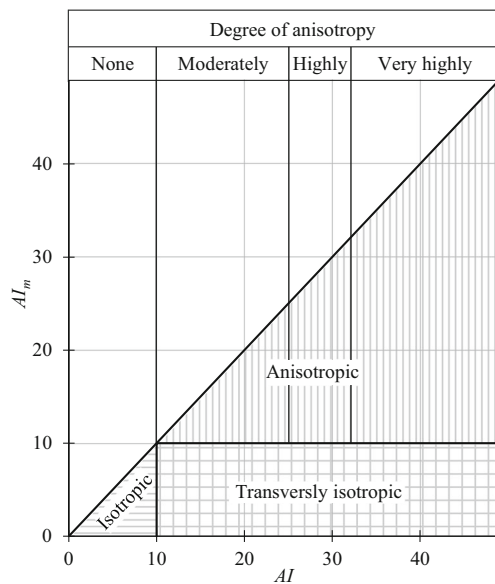


Fig. 10 Identifying the suitable rock mass structural model based on DRMR’s anisotropy indices

Substituting Eqs. 38 and 39 in Eq. 34 yields:

$$R_{cm} = e^{\left(\frac{DRMR^{max}-DRMR^{min}}{18}\right)} \tag{40}$$

Equation 50 shows that the variations of the uniaxial compressive strength of an anisotropic rock mass are proportional to an exponential function of the difference between the maximum and the minimum values of DRMR. Therefore, the anisotropy index, *AI*, based on DRMR can be defined as:

$$AI = DRMR^{max}-DRMR^{min} \tag{41}$$

where its relationship with *R_{cm}* is as follows:

$$AI = 18 \ln R_{cm} \tag{42}$$

Substituting the *R_{cm}* by the lower and upper limits of Ramamurthy’s anisotropy classification and by some modifications to involve the inherent accuracy level of rock mass rating, a classification of the degree of anisotropy of the rock mass based on DRMR is proposed (Table 6).

On the other hand, the rock mass structural models could be divided into three groups: isotropic, transversely isotropic, and anisotropic. With regard to the nature of three-dimensionality of the DRMR, it is rational to establish a criterion to identify and select a suitable rock mass structural model. For this purpose, in addition to the predefined *AI*, an anisotropy index of average DRMR, *AI_m*, is defined as follows:

$$AI_m = \min[(DRMR^{max}-DRMR^{ave}), (DRMR^{ave}-DRMR^{min})] \tag{43}$$

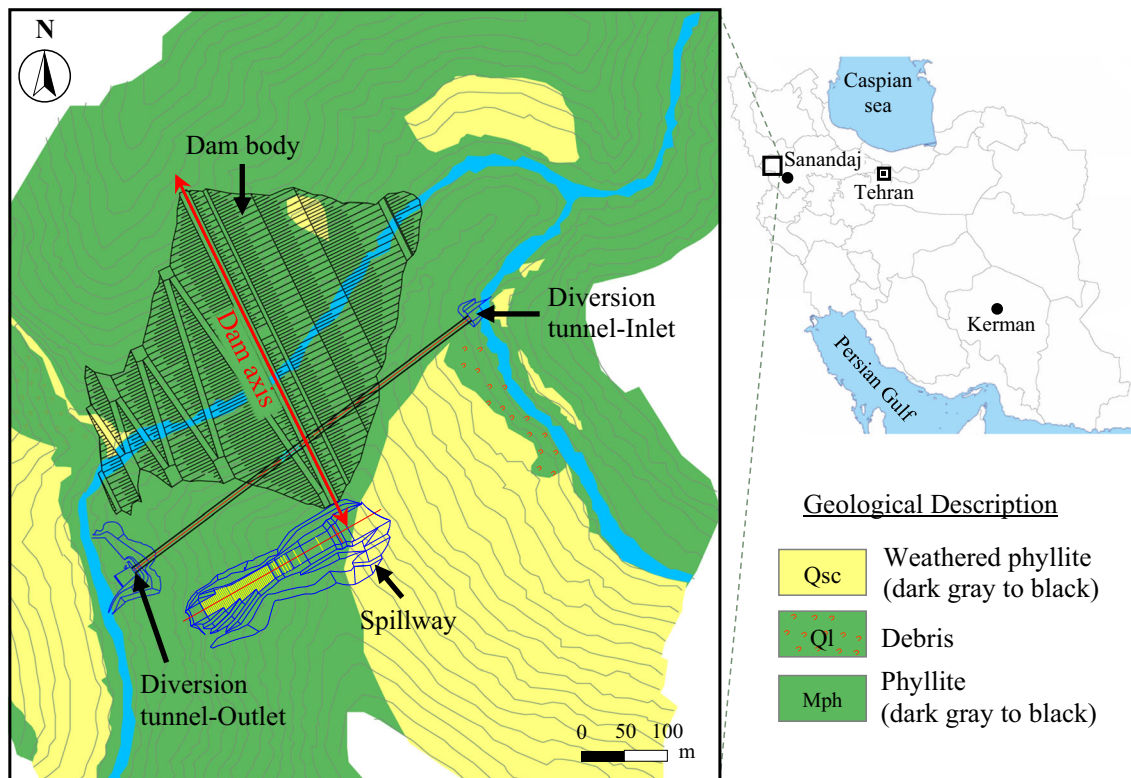


Fig. 11 General layout and geological situation of Kanigoizhan dam site in northwest of Iran (STP 2018)

Table 8 Specifications of discontinuities at Kanigoizhan dam site, northwest of Iran (STP 2018)

Discontinuity set	Dip dir.	Dip	Spacing (m)	Persistence (m)	Aperture (mm)	Roughness	Infilling	Weathering	Joint water
Foliation	042	35	<0.06	3–10	<0.1	Smooth	-	Slightly	Dry
JS1	233	69	0.25	3–10	<0.1	Slightly rough	Soft<5mm	Slightly	Damp
JS2	345	62	0.35	1–3	0.1–1	Slightly rough	Soft<5mm	Slightly	Damp
JS3	119	44	0.35	1–3	0.1–1	Rough	Soft<5mm	Slightly	Damp

where $DRMR^{ave}$ is the average value of DRMR in all-round directions. Accordingly, a criterion is proposed to identify the correct rock mass structural model by using AI and AI_m (Table 7). The graphical representation of this criterion is depicted in Fig. 10. It is worth noting that, in the case of transversely isotropic rock mass behavior, the isotropic plane(s) is perpendicular to the direction of the maximum/minimum DRMR, for which the AI_m has been determined.

Practical applications

An illustrated example

To illustrate the calculation procedure and application of DRMR in describing rock mass anisotropy as well as its

validation, a practical example is given by detail in this section. In this case, the intact rock’s inherent anisotropy and the discontinuities’ induced anisotropy are considered. The field data are taken from Kanigoizhan dam site, under study to be constructed in northwest of Iran. This earth dam with a height of 122 meters from the foundation will have a reservoir capacity of 133 million m^3 . General layout of the dam and its components as well as the geological map of the dam site is depicted in Fig. 11. As it can be seen from this figure, the dam site is mainly composed of Cretaceous metamorphic phyllites, which is the oldest rock unit in this area. The thickness of surface soil layer and weathered zone is generally low. Actually, the phyllites are exposed in a large portion of the site. The phyllites are foliated due to metamorphosis processes.

Table 9 Results of calculation of $DR1_i$ – $DR3_i$ for phyllite rock mass of Kanigoizhan dam site, Iran, along the axes of global Cartesian coordinate system

a) Calculation of UCS_i and $DR1_i$									
Direction (i)	θ_i^p (deg)	UCS_i (MPa)				$DR1_i$			
X	67	27				4			
Y	65	26				4			
Z	35	28				4			
b) Calculation of fracture frequency, λ_i , and $DR2_i$									
Direction (i)	λ_i^F	λ_i^{J1}	λ_i^{J2}	λ_i^{J3}	λ_i	$DR2_i$			
X	3.0	0.7	1.7	7.7	13.1	19			
Y	2.3	2.5	1.0	8.5	14.2	19			
Z	1.5	1.4	2.0	16.4	21.2	14			
c) Determination of discontinuity condition rating (CR^k)									
Discontinuity set (k)	Persistence	Aperture	Roughness	Infilling	Weathering	CR^k			
F (foliation)	2	5	1	2	5	15			
J1	2	5	3	2	5	17			
J2	4	4	3	2	5	18			
J3	4	4	5	2	5	20			
d) Calculation of directional condition rating of discontinuities (CR_i^k) and $DR3_i$									
Direction (i)	θ_i^k	θ_i^{JS1}	θ_i^{JS2}	θ_i^{JS3}	CR_i^k	CR_i^{J1}	CR_i^{J2}	CR_i^{J3}	$DR3_i$
X	42	77	53	76	23	28	21	17	17
Y	56	31	70	65	16	30	23	16	16
Z	69	76	65	35	19	18	30	27	18

The strength anisotropy of the abovementioned phyllites has been well characterized by a set of 37 laboratory tests. The results of these tests were evaluated by the authors, and the spatial distribution of uniaxial compressive strength of the intact phyllite rock was assessed (Maazallahi and Majdi 2020). The resultant equation in compliance with EQ.1 of Table 4 is as follows:

$$UCS_i = 38.6 + 13.3 [\cos^2(35 + \theta_i^{ip})] \quad (44)$$

In addition to foliations, 3 joint sets have been identified in the dam site. The discontinuities' characteristics have been investigated by geological mappings on ground surface and inside of exploration galleries, as well as cores obtained from exploratory boreholes. The discontinuities' characteristics were the same on the left and the right abutments and are presented in Table 8.

Calculation procedure of DRMR

The calculations and the results for DRMR and its 5 components for the current case study are presented in two formats: 3D directions to represent X , Y , and Z Cartesian axes and continuous all-round distribution. The DRMR calculation procedures are given in a "step by step" manner hereafter.

Step 1: To calculate DR1, UCS of the intact rock must be obtained along the prescribed directions. By the procedure and equations given in Table 4 (EQ.1-EQ3), firstly the angles θ_i^{ip} between the isotropic planes of intact rock and the X , Y , and Z axes and then their corresponding UCS_i have been calculated. Consequently, the DR1 _{i} along the mentioned axes has been obtained. The results are presented in Table 9a.

On the other hand, to achieve the contour plot of DR1, the selected network to cover all possible directions consists of trend values from 0 to 360° and plunge values from 0 to 90°, with an interval of 5°. Thus, for each node of the network which is representing a prescribed direction, θ_i^{ip} can be calculated by using EQ.2 of Table 4. Then, UCS_i is calculated for different nodes of the trend-plunge network through Eq. 44. The contour plot of the directional uniaxial compressive strength as well as its corresponding rating, DR1, is depicted in Fig. 12a. According to this figure, DR1 varies between 3 and 5 on different directions.

Step 2: To calculate DR2 _{i} at first, by using Eqs. 14, 15, and 16, the directional linear frequencies of each discontinuity set, λ_i^{JS1} and λ_i^{JS2} , in X , Y , and Z directions are calculated. Then, by using Eq. 17, the cumulative

linear frequency, λ_i , is calculated for each direction. It must be noted that EQ.4 of Table 4 summarizes these calculations to one step. Then, based on the calculated λ_i , DR2 _{i} is calculated by using EQ.5 of Table 4. The results are presented in Table 9b.

Furthermore, DR2 can be calculated for the all-round space through the same computational procedure given in step 1. Contour plot of fracture frequency and its corresponding rating is depicted in Fig. 12b. This figure shows that DR2 varies from 11 to 28 in different directions.

Step 3: To calculate DR3 _{i} , at first, by using the discontinuity specifications data given on Table 8, the values of condition rating for each discontinuity, CR^k , are obtained based on Table 3. The results are reported in Table 9c. Then, using EQ.6-EQ.8 of Table 4, the directional ratings for each discontinuity CR_i^k and finally DR3 _{i} are calculated (Table 9d). Following the same procedure as given in step 1, the contour plots of DR3 have been drawn and shown in Fig. 12c.

Step 4: To calculate the last rating component, DR4 _{i} , with regard to the general water conditions of the discontinuity sets (Table 8), the values of JWC^k are determined equal to 15 and 10 for foliation and joint sets, respectively. Then, using EQ.7 and EQ.9-EQ.10 of Table 4, the directional joint water condition ratings for each discontinuity JWC_i^k and finally DR4 _{i} are calculated. These calculations yield the same value of 15 for DR4 _{i} along X , Y , and Z directions. Following the same procedure as given in step 1, the contour plots of DR4 have been drawn and shown in Fig. 12d. This figure illustrates that the all-round distribution of DR4 varies from 10 to 15.

Step 5: Finally, DRMR is calculated by summing up the rating values of DR1 to DR4 and is summarized and presented in Table 10. Also, the maximum, the minimum, and the average values of DRMR are reported in the same table, as well. The corresponding contour plot of DRMR is depicted in Fig. 12e. As it can be seen, the maximum and the minimum values of DRMR are 73 and 44, respectively. The calculated anisotropy indices, based in Tables 6 and 7 and Fig. 10, show that the rock mass has a "highly anisotropic" degree of anisotropy and a "transversely isotropic" structural model. Since DRMR is capable to provide all-round rating values, hence, DRMR's highest and lowest values shown in 3D, X , Y , and Z directions, may not be the same as the maximum and the minimum values as shown in Table 10. Based on the data which is presented in this table, one can analyze the role of each rating component in the obtained

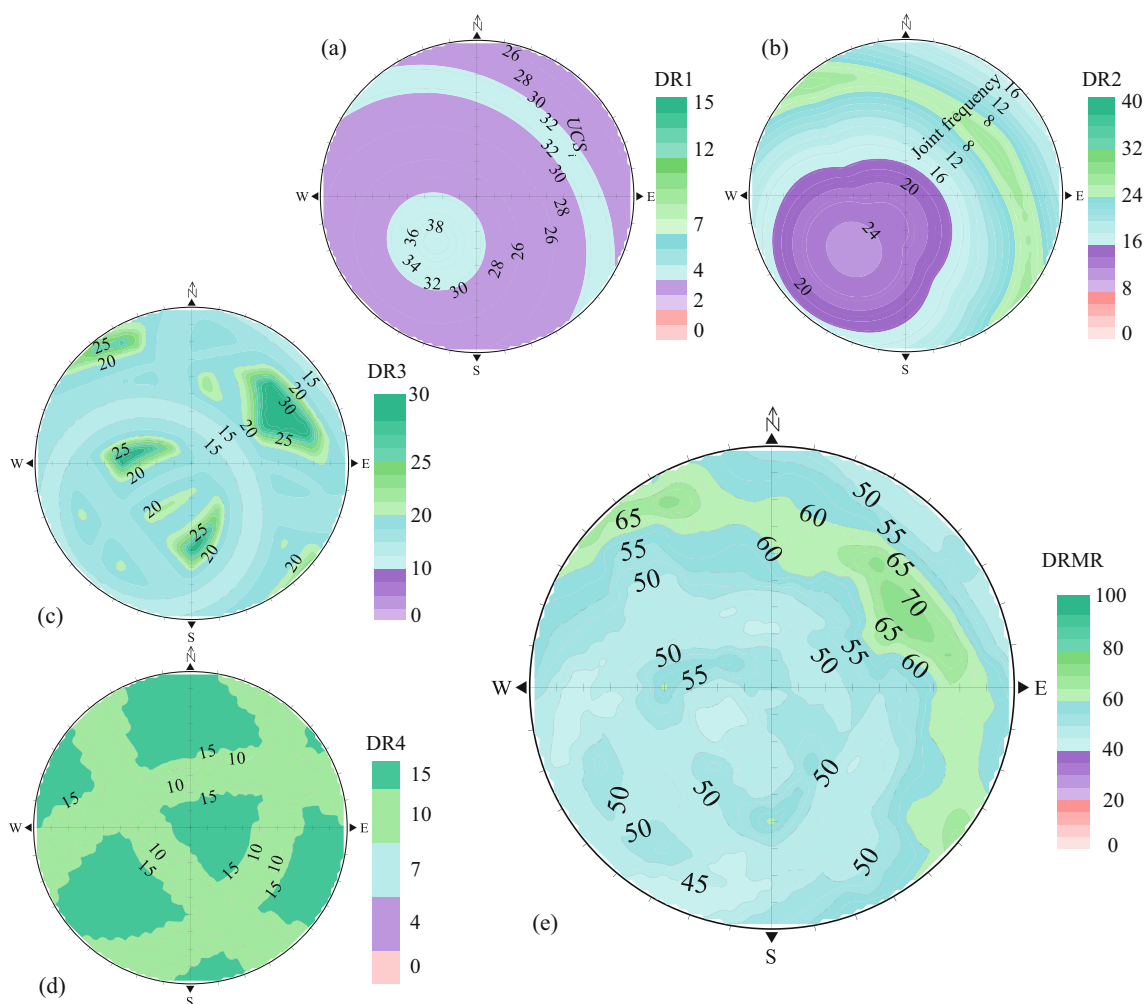


Fig. 12 Contour plots of DRMR and its components for a phyllite rock mass obtained from Kanigoizhan dam site, Iran; **a** $UCSi$ and its corresponding rating, DR1; **b** fracture frequency and its corresponding rating, DR2; **c** discontinuity condition rating, DR3; **d** joint water condition rating, DR4; **e** DRMR

behavior of the rock mass. By comparing the values of DR1–DR4 of the maximum and the minimum DRMR, it can be inferred that, in this case, the DR2

(fracture frequency) and then DR3 (conditions of discontinuities) have the most influential role in the obtained degree of anisotropy.

Table 10 Calculation of DRMR for a phyllite rock mass, obtained from Kanigoizhan dam site, Iran

Description	Rating direction, i (trend/plunge)	Directional rating components				DRMR _{i}
		DR1 _{i}	DR2 _{i}	DR3 _{i}	DR4 _{i}	
DRMR along global Cartesian axes	X	4	19	17	15	55
	Y	4	19	16	15	53
	Z	4	14	18	15	50
Max. DRMR	330/10	4	27	28	15	73
Min. DRMR	240/65	4	12	17	10	44
					DRMR ^{ave}	52
					AI	29
					AI_m	9
					Rock mass behavior	Highly anisotropic

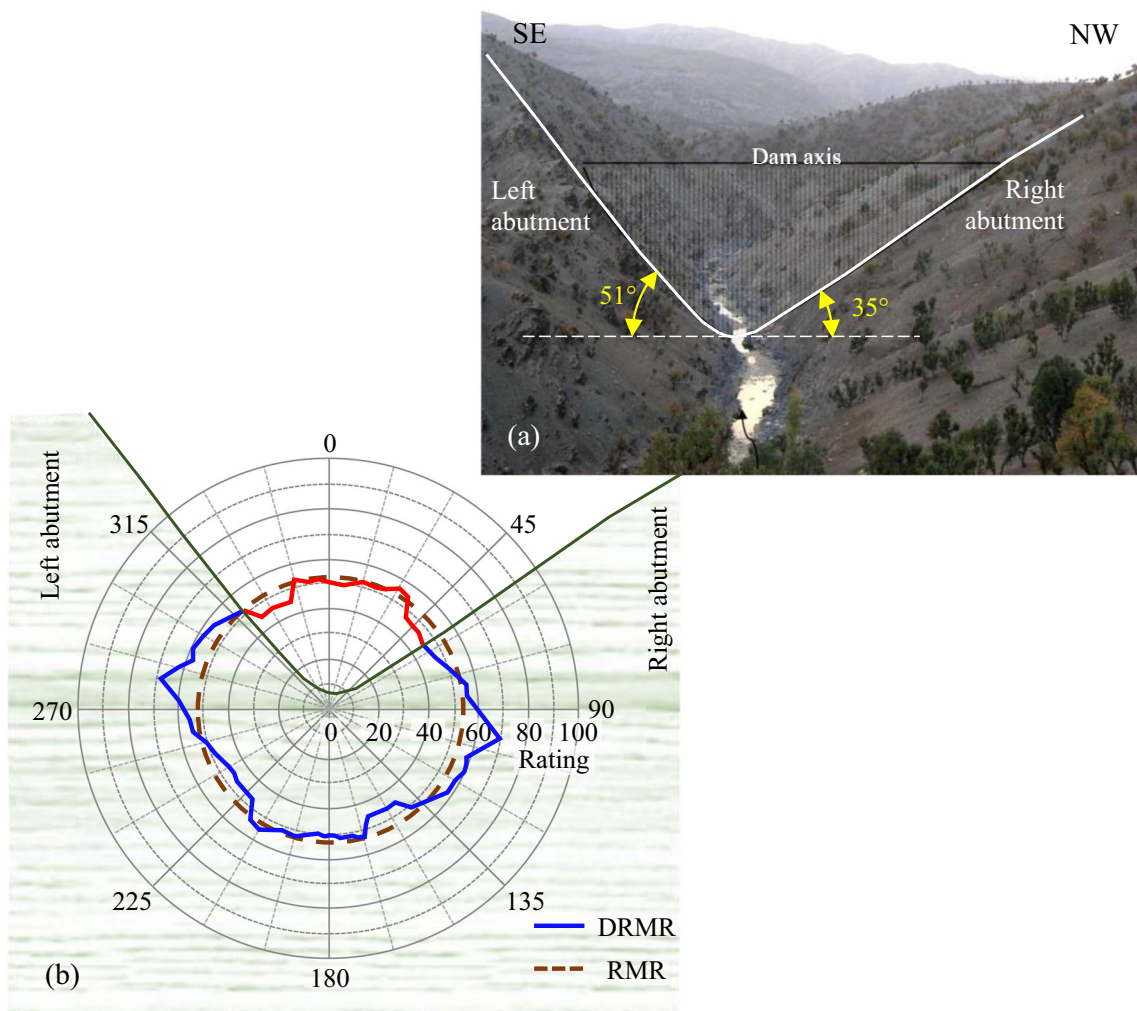


Fig. 13 The natural situation of the Kanigoizhan dam abutments (a) and their compliance with the directional rock mass rating, DRMR (b) in a cross section along the dam axis (view to downstream)

Validation of DRMR

Based on the results obtained for the Kanigoizhan dam site which were presented in the previous section, a study has been done to evaluate the validity of DRMR. For this purpose, the correlations between DRMR and condition of natural slopes and tunnel wall displacements have been investigated and will be described hereafter.

As mentioned before, the thickness of the soil layers on the dam site is generally low, and phyllites outcrop on the natural

slopes. Thus, geomorphology of the site is largely affected by the quality of the phyllite rock mass. To evaluate this relation, a cross section along the dam axis has been selected and investigated. A picture of this section is shown in Fig. 13a. This picture shows that the natural slope of the dam abutments on its right and left sides is significantly different. While the ground slope on the right abutment is 35°, it is 51° on the left abutment. To evaluate the correlation of this difference with the directional rock mass rating, the 2D diagram of DRMR is prepared in the same section and is presented in Fig. 13b. According to this diagram, DRMR varies from 45 to 73 which implies the anisotropic behavior of rock mass at this section. The natural slope of the dam abutments is also depicted on this diagram. Comparison of DRMR values at the 2 opposite abutments shows that the DRMR values on the left abutment are clearly higher than that on the right abutment. On both abutments, it can be seen that the natural slope of the ground surface is located at an angle where the DRMR is about 50. However, the angle which exhibits this rating on the left

Table 11 Parameters of transversely isotropic phyllite of Kanigoizhan dam site used for numerical analysis (STP 2018)

m_b	s	σ_{ci} (MPa)	E_1 (GPa)	E_2 (GPa)	G_{21} (GPa)	ν_1	ν_{21}
1.17	0.0038	50	81	27	16.5	0.45	0.15

abutment is more than the right abutment ones. Therefore, it can be concluded that DRMR is in good agreement with the stability and natural slope of the rock slopes in the studied area. Furthermore, a comparison has been made between the calculated DRMR and conventional RMR on this section. On this section, the rating adjustment for joint orientations (Table 1) is zero due to the right angle between the strikes of slope and foliation. Hence, its RMR is equal to 53. This comparison clearly shows the advantages of DRMR than RMR.

Since the Kanigoizhan dam has not been completed until the present study, there is naturally no monitoring or field data available on the rock mass response to the construction of the structures. Hence, the behavior of an access tunnel of the project has been simulated by numerical modeling and used for further validation of DRMR. This tunnel has been designed along the direction of N50W-S50E to access to the dam crest. Since the tunnel axis is parallel with the strike of foliations, a 2D analysis can be adopted. For this purpose, *Phase²* finite element code has been used. Thus, numerical modeling and analysis were performed in a cross section perpendicular to the foliations (i.e., N40E-S40W). In order to

avoid the complexity of the analysis and to eliminate the effect of various parameters on the results, a circular tunnel cross section (with an equivalent radius of 4.25 m), elastic rock mass behavior, and hydrostatic stress field have been considered. Accordingly, for the prescribed goal, the elastic displacements on the tunnel wall will be compared with the corresponding DRMR distribution.

Rock mass parameters used for numerical analysis have been obtained from laboratory and field tests and are summarized in Table 11. Figure 14a shows the displacement contours obtained from the numerical analysis. Also, the 2D diagram of DRMR along the modeled section has been prepared and is presented in Fig. 14b. Comparison of these 2 figures shows that there is a good agreement between the tunnel wall displacements obtained from the numerical model and the variations of the directional rock mass rating. So, the highest tunnel wall displacements occurred in directions where DRMR diagram exhibits its lowest values. In comparison, in the directions with a higher DRMR, the tunnel wall displacements are smaller. Hence, there is a good reverse correlation between DRMR and tunnel wall displacements. Again, a comparison

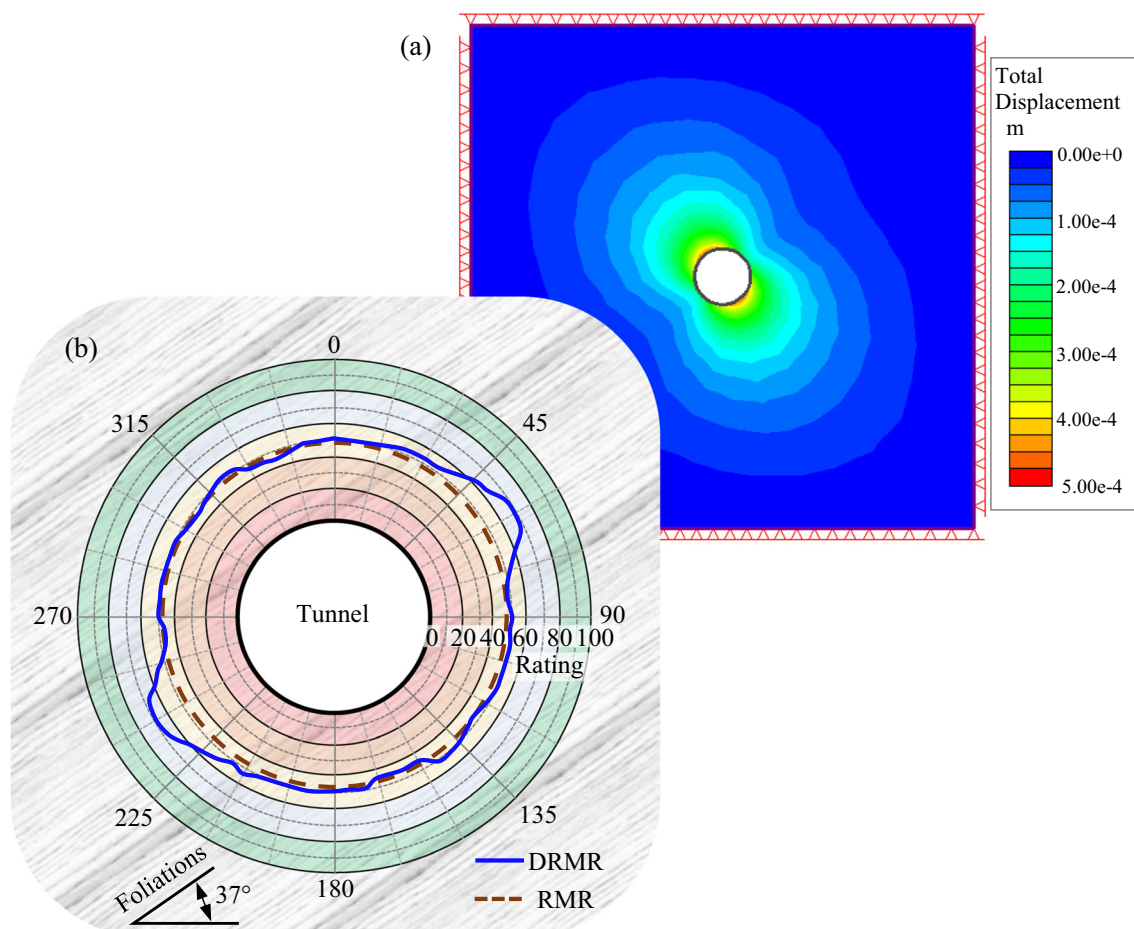
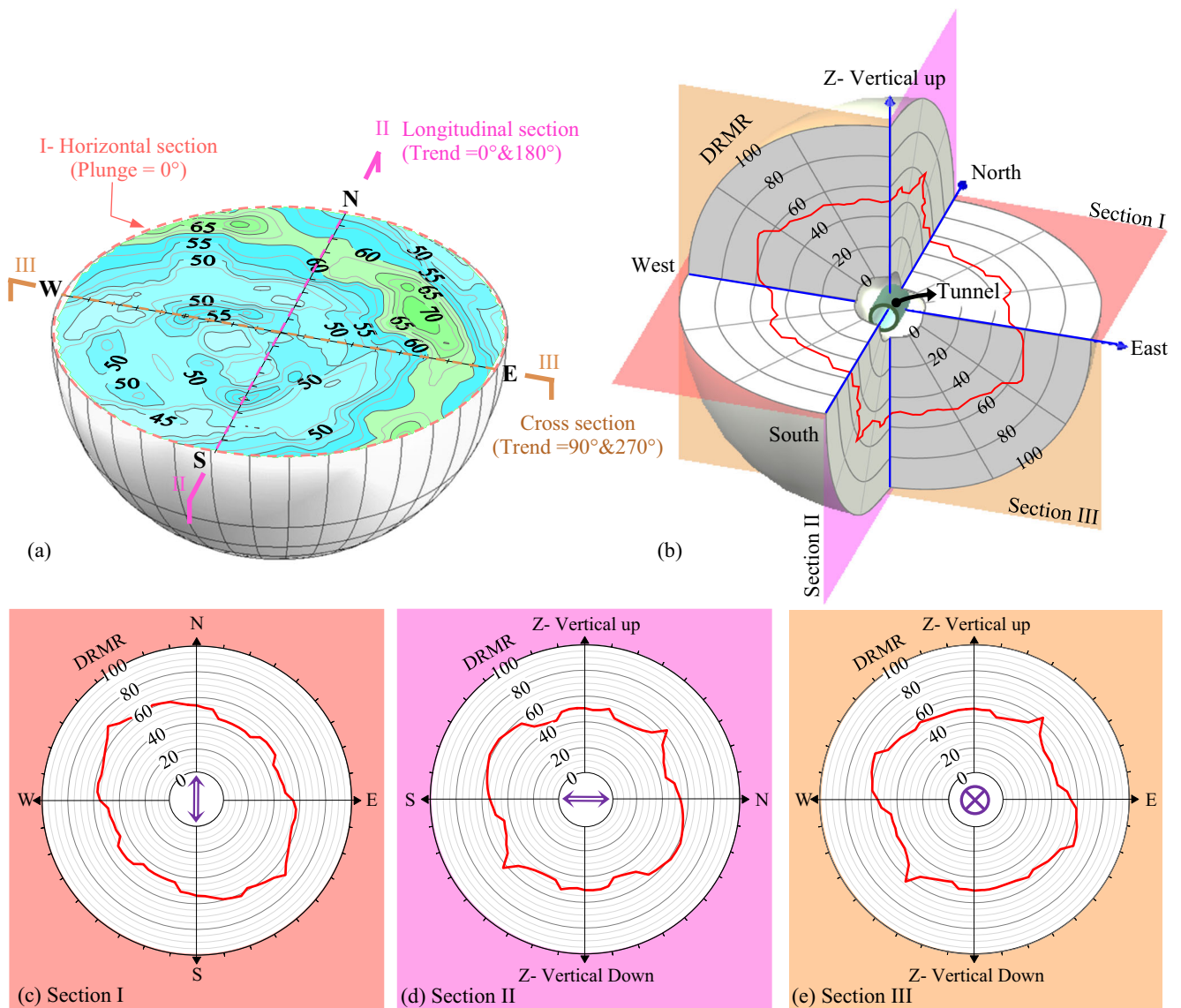


Fig. 14 Comparison of elastic displacements of tunnel wall with directional rock mass rating; **a** displacement contours obtained from numerical modeling, **b** 2D diagram of DRMR along the same cross section



* The tunnel alignment is shown on the middle circle of diagrams.

Fig. 15 Detailed illustration of DRMR; **a** alignment of 2D diagrams on DRMR stereonet, **b** 3D block representing distribution of DRMR on three orthogonal sections, **c** 2D distribution of DRMR on a horizontal

section, **d** 2D distribution of DRMR on N-S longitudinal section, **e** 2D distribution of DRMR on E-W cross section

has been made between the DRMR and RMR. On this section, RMR reduces to 48 due to the “fair” effect of foliations’ orientation on tunneling (rating adjustment for joint orientations = -5 based on Table 1). As it can be seen, the proposed DRMR develops the application range of conventional RMR to anisotropic rock mass problems, satisfactorily.

Detailed analysis of DRMR results

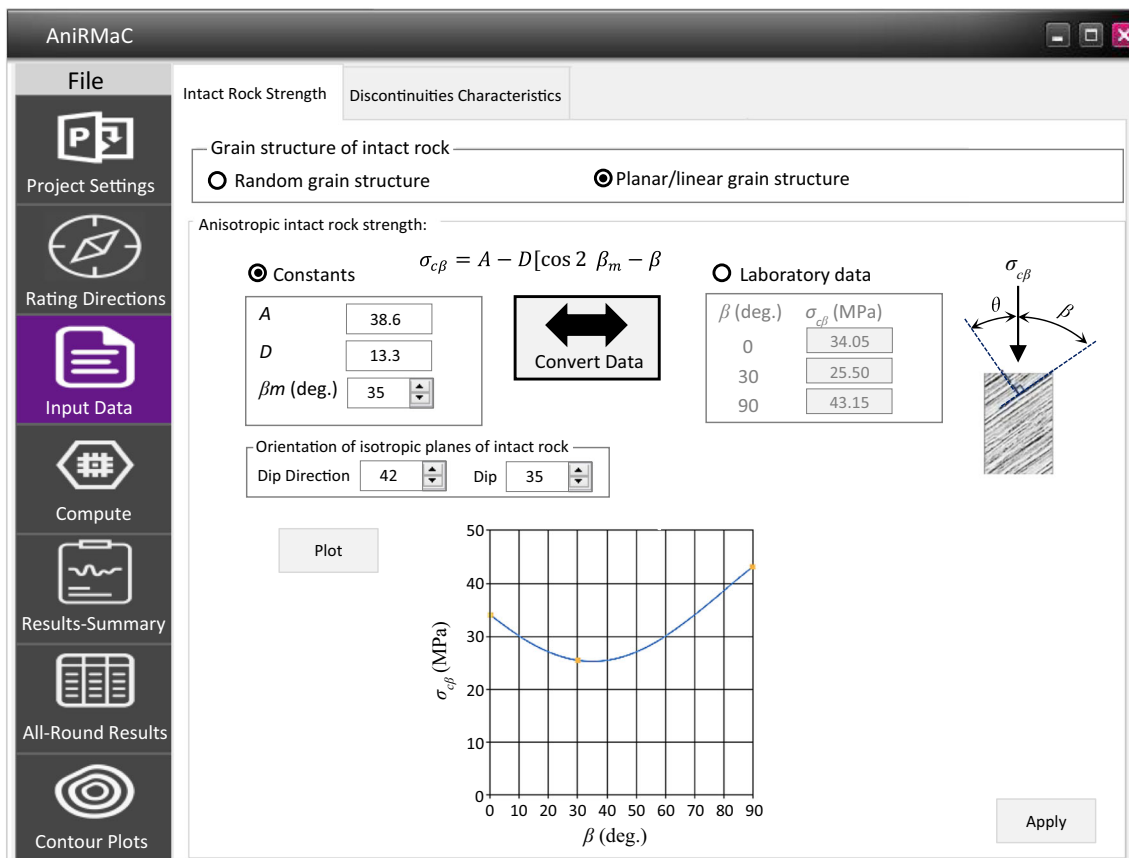
Representation of DRMR in the form of stereonet can assist to determining the tunnel/underground space alignment. This is a practical tool for the case that there is enough flexibility for optimal alignment design of the underground space, e.g.,

caverns. This alignment could be designed in a direction that has the highest DRMR to support the critical stress concentration zone around the tunnel periphery/face. The all-round nature of the stereonet representation can allow the designer to adopt the tunnel alignment with the anisotropy condition of the rock mass. However, more detailed investigations could be arranged by providing 2D diagrams of DRMR variations on desired directions. For example, Fig. 15 shows the DRMR’s distribution of the current example as 2D diagrams on three orthogonal planes (Fig. 15a and b): horizontal section (I), longitudinal section parallel with a grouting gallery on the right abutment (II), and cross section perpendicular to the mentioned grouting gallery (III). Figure 15c illustrates that

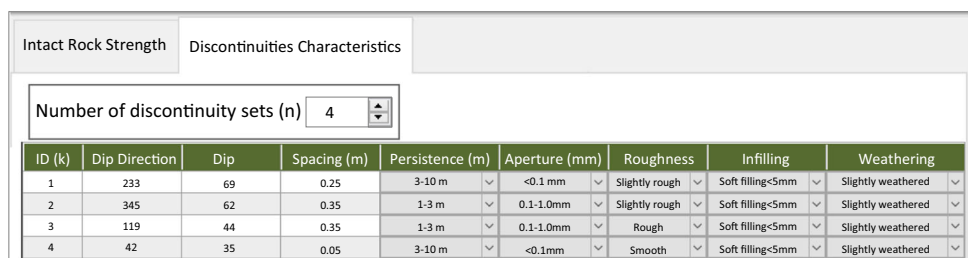
the N40W and S40E directions represent the highest DRMR on the horizontal plane (plunge=0). Such a graph can be used to design the optimal alignment for an underground structure which must be built with no slope. For an optimal design, such an underground space has to be positioned so that the locations of stress concentration on its periphery lay on the directions of highest DRMR. Two other graphs are provided for vertical sections parallel with (Fig. 15d) and perpendicular to (Fig. 15e) the mentioned tunnel axis. These graphs can be used to distinguish the weaker zones around the tunnel periphery/face, in the first place, and then to take the necessary stability measures, such as adopting the support system that matches the actual rock mass conditions, as a selective rock mass improvement.

AniRMaC code for DRMR calculations

To facilitate the calculation procedure of DRMR and obtain the results in the mentioned formats, a windows form code has been developed. This code, which is termed AniRMaC, takes the input parameters and supplies the results through a user-friendly GUI and in a stepwise manner. A dashboard is embedded on the home screen that allows the user to control and use different parts of the program. To use the AniRMaC code, after setting the project details and rating directions, the input parameters must be entered in two categories of intact rock strength and discontinuities' characteristics (Figs. 16a, b, respectively). Then, the results can be calculated by clicking on the "Compute" button. The program provides the results in



(a)



(b)

Fig. 16 AniRMaC windows form code for detailed DRMR calculations; **a** program dashboard and input data-intact rock strength; **b** input data-discontinuities' characteristics. The data are taken from the example of the section "An illustrated example"

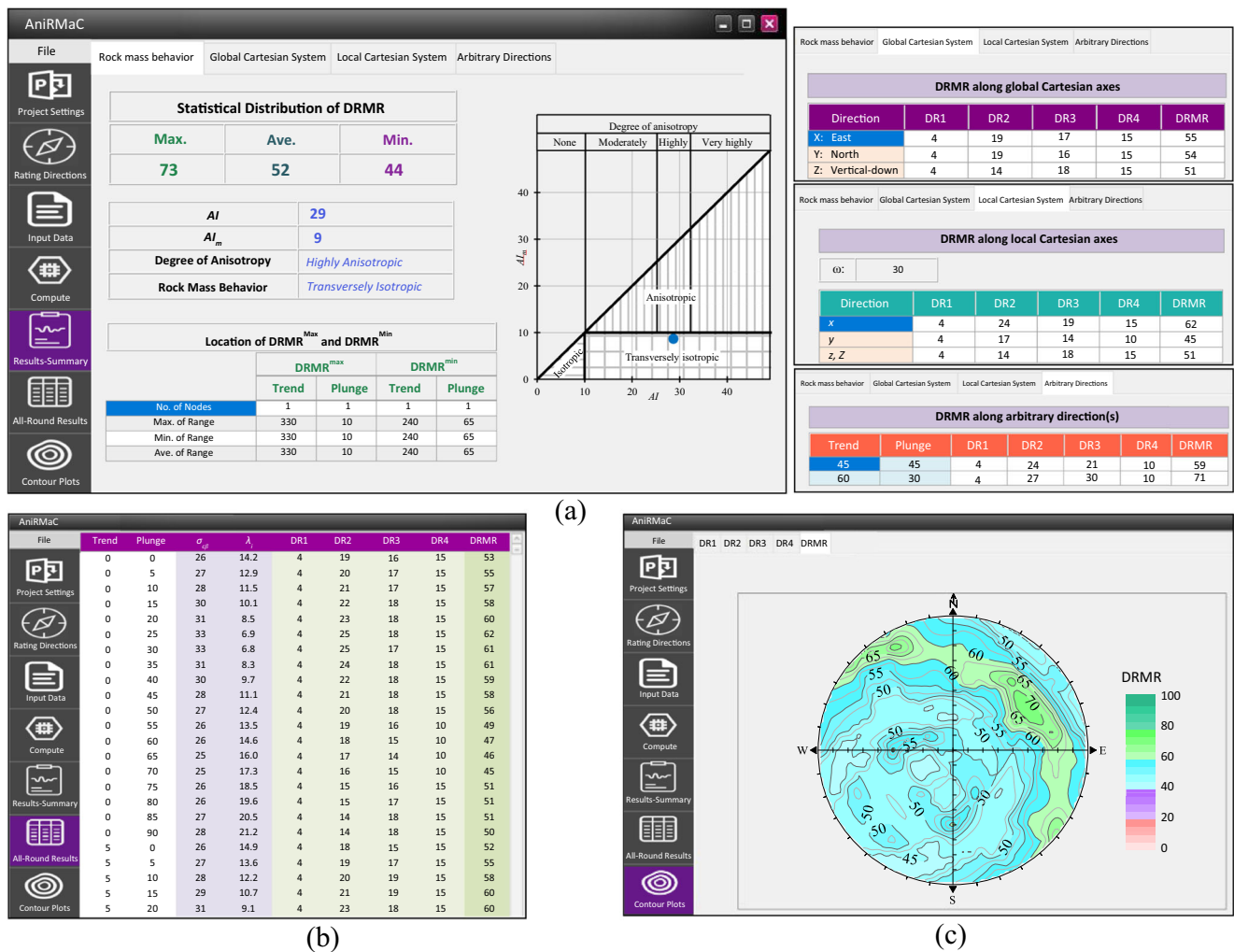


Fig. 17 Results of application of AniRMaC code for the example of the section “An illustrated example”; **a** summarized results, **b** all-round results, **c** contour plot of DRMR

3 different formats. “Results-Summary” tab provides the rock mass behavior in terms of statistical distribution of DRMR, AI and AI_m . It also provides DRMR and its components along with the global and local Cartesian axis and also the user-defined arbitrary directions. The results of calculations for each node of the trend/plunge network are available on “All-Round Results” tab. Finally, the contour plots of DRMR and its components are accessible via the “Contour Plots” tab. The results of application of the code for the example given in the section “An illustrated example” is shown in Fig. 17.

Examination of DRMR performance in different rock mass conditions

To evaluate the applicability of the proposed DRMR method in facing with different rock mass conditions, further field data obtained from dam and tunnel projects in Iran have been analyzed. The geographical locations of selected projects are

shown in Fig. 18. A brief description of each case is outlined in the following.

Rudbar-e-Lorestan D&HPP: Rudbar-e-Lorestan earth embankment dam and hydropower plant, located 92 km south of Aligoudarz city, Lorestan province, Iran. The dam foundation and its abutments consist of Dalan geological formation, which is composed of alternations of limestone and dolomite-limestone layers with variable thicknesses. The dam site has been divided into 8 zones from geological and geotechnical point of view (IWPCO 2007). However, the required data obtained from 4 of these zones are used in this section. Since the dam abutments are oriented along a direction of N30E, a local coordinate system is defined with the angle of rotation, $\omega=30^\circ$, to determine DRMR.

Karun-IV D&HPP: The Karun-IV concrete dam and hydropower plant (D&HPP), located in Chaharmahal-o-Bakhtiari province, Iran, 180 km from south and southwest of Shahrekord

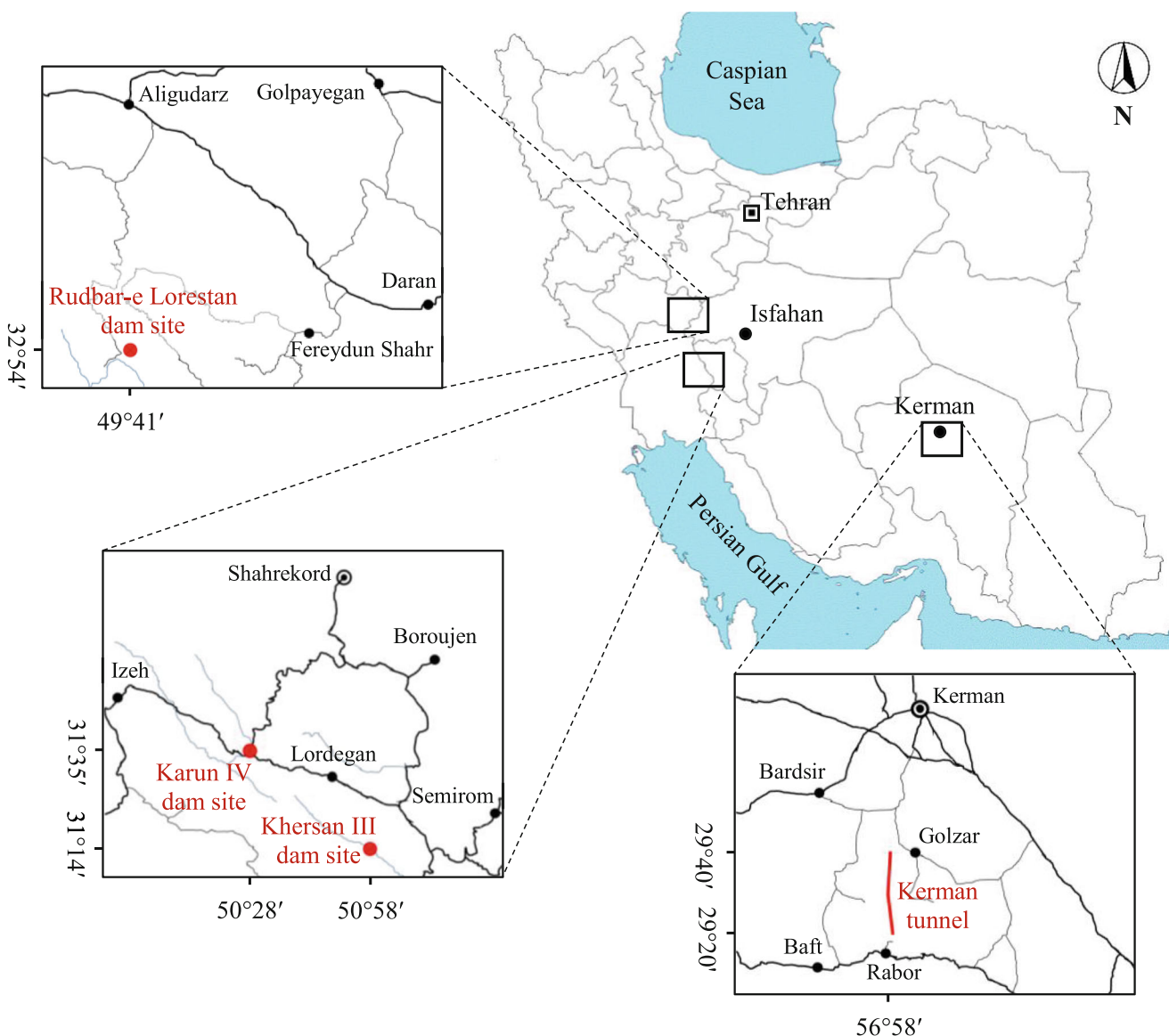


Fig. 18 The geographical location of selected dam and tunnel projects from Iran as case studies

city. Geological mapping data are obtained from LG2 grouting gallery that has been excavated with azimuth 70° through As_1 member of Asmari geological formation. This zone generally consists of a thick layered, strong limestone. In addition to bedding planes, there are three main joint sets in this zone (IWPCO 2004).

Kherasan-III D&HPP: Kherasan-III double curvature arch dam and hydropower plant, located 50 km southeast of Lordegan city, Chaharmahal-o-Bakhtiari province, Iran. The diversion tunnel of the project has been excavated with a diameter of 12.6 meters and a length of 725 meters with a variable azimuth ranging from 220 to 320° from inlet to outlet, respectively. The tunnel passes through the lower Asmari formation, which consists of marl-limestone and dolomite (IWPCO 2010).

Kerman WCT: Kerman water conveyance tunnel with a length of 38 km is under construction to transfer drinking water from Safarood dam to Kerman city, the center of the widest province of Iran. The tunnel passes through the south and southeastern mountains of Kerman at a depth of 50–950 m along an almost N-S alignment. A large portion of the tunnel route passes through igneous and metamorphic formations. These formations are composed of different rock types, mainly including alternations of units of basalt, andesite, tuff, and basaltic andesitic lava flows. Also, limestone, sandstone, and shale units are observable in some areas (KRWA 2016). The tunnel, longitudinally, is divided into different zones based on the regional geology. Data obtained from the three zones have been used for DRMR determination.

Table 12 Field data obtained from Iranian sites (Fig. 19) used to evaluate the credibility of DRMR

Project	Zone	Rock type	UCS (MPa)	Discontinuities' characteristics				Aperture (mm)	Roughness*	Filling	Weathering**	Joint water Condition	
				ID	Dip dir.	Dip Persistence (m)	Spacing (m)						
Rudbar-e-Lorestan	Zone A	Limestone-dolomite limestone	65-80	J1	140	82	9	0.15	Und., R.	Stain	M.	Dry	
				J2	230	82	7	0.35	Und., R.	Stain	Sl.	Dry	
				J3	329	82	10	1.6	Und., R.	Stain, loam	Sl.	Dry	
	Zone B		65-80	B	70	63	20	0.6-2	Und., R.	Loam	Sl.	Dry	
				J1	230	61	7	0.8	Und., R.	Stain	M.	Dry	
				J2	50	61	4	0.6	Und., R.	Stain	Sl.	Dry	
	Zone D		65-80	J3	208	53	3	0.5	Und., R.	Stain, loam	Sl.	Dry	
				B	300	72	4	0.6	Und., R.	Loam	Sl.	Dry	
				J1	270	60	20	0.5	Und., R.	Stain	Sl.	Dry	
				J3	310	82	12	1.0	Und., R.	Bitumen, loam	Sl.	Dry	
Karun-IV	LG2 gallery	Limestone	62	B	210	77	30	0.2	Pl., R.	Bitumen	Sl.	Dry	
				J1	325	68	7	2	0.25-0.5	St., R.	Stain	Sl.	Dry
				J2	299	57	7	0.3	0.25-0.5	Und., R.	Stain	Sl.	Dry
				B	226	82	25	1.3	0.25-1	St., R.	Stain, loam	Sl.-M.	Dry
				B	215	70	>20	1.8	1-2	Und., R.	Calcite	Fr.	Dry
Khersan-III	Diversion tunnel	Dolomite	61-74	J1	315	75	10-15	0.5	Und., R.	-	Sl.	Dry	
				J2	120	75	7-10	1.4	10	Und., R.	Marl	M.-H.	Dry
				J3	80	70	3-5	0.8	3	Und., R.	Calcite	M.	Dry
				B	055	50	>20	0.6-2	>10	Und., S.	Calcite	Fr.	Dry
				J1	270	70	3-10	0.2-0.6	0.5-5	Pl., S.	Calcite	Fr.	Dry
Kerman tunnel	KT_Z1	Andesite	160-200	J2	240	45	1-3	0.2-0.6	Pl., S.	-	M.	Dry	
				J3	310	75	3-10	0.06-0.2	0.5-2	Pl., S.	Marl	Sl.	Dry
				J4	125	25	3-10	0.2-0.6	1-5	St., Sl.	Calcite	H.	Dry
				J1	163	85	3-10	0.8	1.5-2	R.	None	Fr.	Wet-dripping
				J2	359	80	3-10	0.8	1.5-2	Sl. S.	None	Fr.	Wet-dripping
	KT_Z2	Andesite	90-120	J3	268	67	1-3	2.0	<0.5	Sl. S.	Fr.	Wet-dripping	
				J1	115	75	3-10	0.4	0.5	R.	None	Fr.	Wet-dripping
				J2	120	50	3-10	0.7	0.2	St. S.	None	M.	Dripping
	KT_Z3	Andesite	90-120	J3	000	50	3-5	0.6	0.5	R.	None	Dripping	
				J1	255	70	3-10	0.9	0.5-1	R.	Hard filling	Sl.	Wet
				J2	025	75	1-3	0.5	Pl., R.	None	Sl.	Wet	
				J3	235	35	3-10	0.6	R.	None	Sl.	Wet	

*Und., undulating; St., stepped; Pl., planar; R., rough; S., smooth; Sl., slickensided
 **Fr., fresh; Sl., slightly weathered; M., moderately weathered; H., highly weathered

Table 13 DRMR calculated based on field data shown in Table 12

Project	Zone	$DRMR_i$			Max. DRMR		Min. DRMR		$DRMR^{ave}$	AI	AI_m	Rock mass behavior
		x	y	z	Value	Trend/plunge	Value	Trend/plunge				
Rudbar-e-Lorestan D&HPP	Zone A	58	58	64	82	234/21	58	(190 and 310)/25	66	24	8	Trans. isotropic
	Zone B	73	82	68	82	*	64	*	69	18	5	Trans. isotropic
	Zone D	76	64	68	92	265/68	55	*	66	37	11	Highly anisotropic
	Zone E	79	71	73	92	334/56	66	*	74	26	8	Trans. isotropic
Karun-IV D&HPP	LG2 gallery	60	60	71	87	045/55	60	*	67	27	7	Trans. isotropic
Khersan-III D&HPP	Diversion tunnel	53	48	51	56	-	48	-	52	8	-	Isotropic
Kerman tunnel	KT_Z1	74	76	75	86	270/75	63	*	74	23	11	Moderately anisotropic
	KT_Z2	61	60	60	76	045/55	58	*	63	18	5	Trans. isotropic
	KT_Z3	65	68	67	75	-	66	-	68	9	-	Isotropic

*In these cases the max/min value of DRMR is observed on a wide range of directions; hence, a single direction cannot be stated to describe it

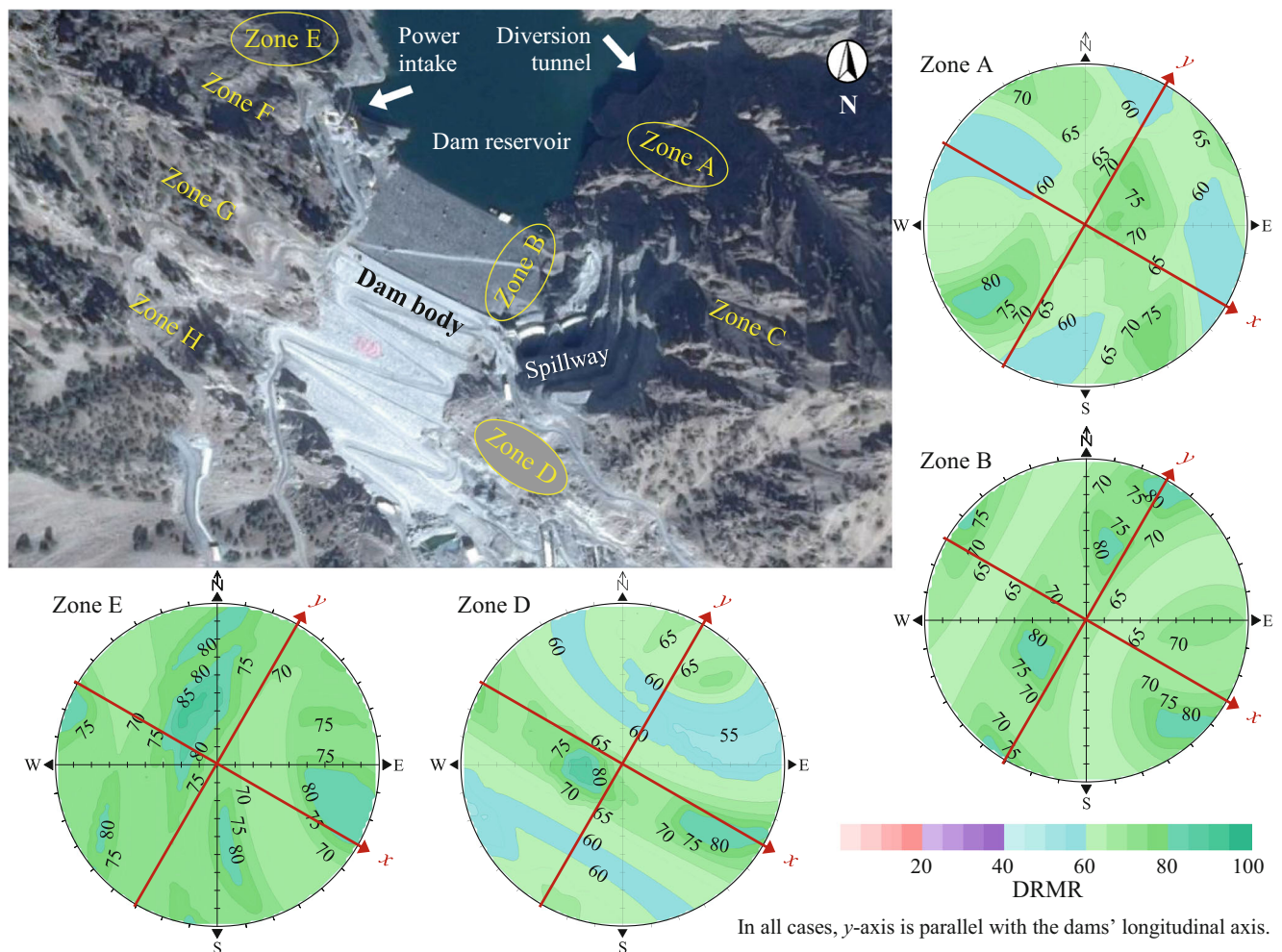


Fig. 19 Contour plots of DRMR for 4 geological zones of Rudbar-e-Lorestan dam site, Iran

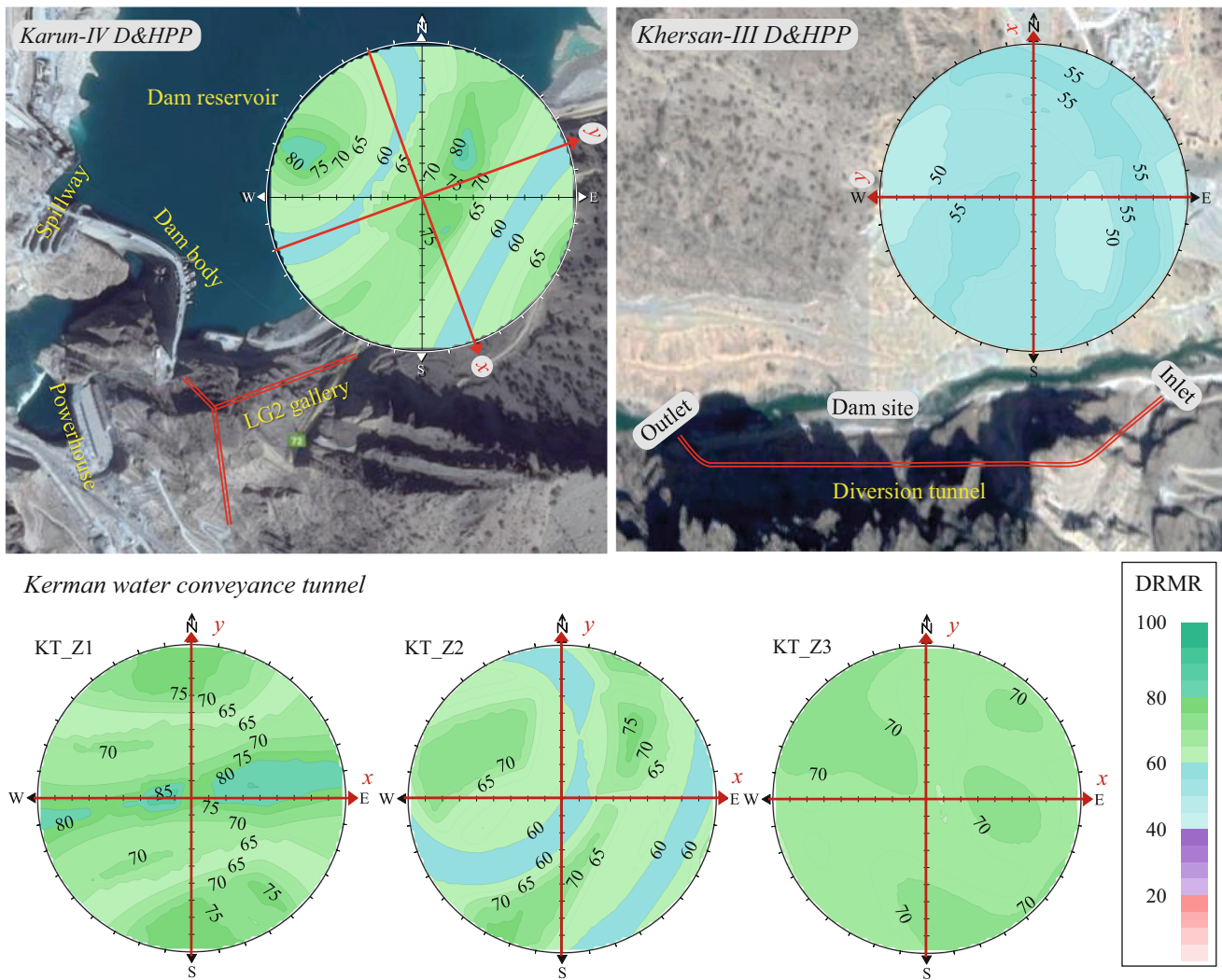


Fig. 20 Contour plots of DRMR for 3 case studies of dam and tunnels from Iran: Karun-IV dam—grouting gallery LG2; Khersan-III dam, diversion tunnel; and Kerman water conveyance tunnel, zones KT_Z1, KT_Z2, KT_Z3

Details of the input data for calculation of DRMR are given in Table 12.

DRMR for the aforementioned cases has been evaluated based on the procedures mentioned in the sections “Directional rock mass rating (DRMR), methodology and development” and “Development of an anisotropy index based on DRMR.” For each case, the local coordinates are defined with regard to geometrical configuration of the structures. Table 13 gives the DRMR values obtained for each case along with its local x , y , and z directions as well as the maximum, the minimum, and the average values of DRMR. Also, based on the calculated anisotropy indices, AI and AI_m , the proper rock mass behavior is presented for each case. The contour plots of DRMR for these cases are illustrated in Figs. 19 and 20. With regard to the results obtained, the rock mass behavior is varying from isotropic to anisotropic depending on the jointing condition of each case.

Conclusion

The very well-known RMR is developed by Bieniawski and generally is used to categorize and evaluate the role of the most significant parameters influencing rock mass behavior to represent an isotropic equivalent continuum. However, almost all rocks, especially metamorphic and sedimentary rocks, and also systematically fractured rocks, exhibit some degrees of anisotropy. Hence, in this paper, RMR has been used as a base to develop a method to represent the rock mass as an anisotropic equivalent continuum. On this basis, a directional rock mass rating (DRMR) has been proposed to take the aforesaid conditions into account. DRMR characterizes the rock mass as an anisotropic medium, so that it is possible to determine the rating of rock mass at any arbitrary direction. One of the most important aspects of the proposed method is that it incorporates both intrinsic anisotropy of intact rock and

the induced anisotropy caused by discontinuities. For proper evaluation of rock mass quality, an all-round presentation has been proposed in the form of DRMR contour plot by means of lower hemisphere stereonet. For further analysis, if needed, the components of DRMR could also be illustrated in a similar manner. Using this type of presentation, along with the directional rock mass rating, can significantly contribute to deal with the rock mechanics and rock engineering issues. The statistical distribution of DRMR, in terms of its maximum, minimum, and average values, gives a worthy view of anisotropy/isotropy of the rock mass. Based on the difference between the maximum and the minimum values of DRMR, an anisotropy index has been proposed to classify the degree of anisotropy of a rock mass. Furthermore, a criterion is presented to identify the isotropic/transversely isotropic/anisotropic situation of the rock mass. The validation of DRMR has been examined by an actual case study. This examination showed that there is good correlation between the calculated DRMR and stability of natural rock slopes, as well as tunnel wall displacements. Comparison of DRMR with RMR clarified that the proposed method provides a significant development within the rock mass classification systems in dealing with rock mass anisotropy. Finally, the data obtained from four other different dam and tunnel sites have been used to evaluate the applicability of DRMR proposed in this paper.

For the cases of transversely isotropic/anisotropic rock masses, the proposed DRMR can be utilized as a base for determination of rock mass mechanical parameters as a transversely isotropic/anisotropic equivalent continuum. Representation of DRMR in the form of stereonet can also be used as a practical tool for the case that there is enough flexibility for optimal tunnel and underground cavern alignment design as well. It provides opportunities to improve the technical and economic aspects of rock engineering designs, such as localized support system and selective rock mass improvement, as well. Each of these potential applications may be affected by other factors, like confining stress, which must be taken into account based on the nature of the under-study problem. Though the final output reflects a very satisfactory measure of the rock quality, quantitatively, however, further applications are recommended to appreciate the applicability and the credibility of the method proposed.

References

- Agricola G (1556) *De re metallica*. Translated from the first Latin edition of 1556 by H.C. Hoover and L.H. Hoover, 1950. Dover Publications, Inc., New York
- Ajalloean R, Lashkaripour GR (2000) Strength anisotropies in mudrocks. *Bull Eng Geol Environ* 59:195–199. <https://doi.org/10.1007/s100640000055>
- Aksoy CO (2008) Review of rock mass rating classification: historical developments, applications, and restrictions. *J Min Sci* 44:51–63. <https://doi.org/10.1007/s10913-008-0005-2>
- Aydan Ö, Ulusay R, Tokashiki N (2014) A new rock mass quality rating system: rock mass quality rating (RMQR) system and its application to the estimation of geomechanical characteristics of rock masses. *Rock Mech Rock Eng* 47:1255–1276. https://doi.org/10.1007/978-3-319-09060-3_137
- Barton N, Quadros E (2014) Most rock masses are likely to be anisotropic. In: *Rock Mechanics for Natural Resources and Infrastructure SBMR 2014 – ISRM Specialized Conference*. CBMR/ABMS and ISRM, Goiania
- Barton N, Lien R, Lunde J (1974) Engineering classification of rock masses for the design of tunnel support. *Rock Mech* 6:189–236
- Bieniawski ZT (1973) Engineering classification of jointed rock masses. *Civ Eng South Afr* 15:343–353. [https://doi.org/10.1016/0148-9062\(74\)92075-0](https://doi.org/10.1016/0148-9062(74)92075-0)
- Bieniawski ZT (1976) Rock mass classification in rock engineering. In: Bieniawski ZT (ed) *A Symposium on Exploration for Rock Engineering*. Cape Town, pp 97–196
- Bieniawski ZT (1979) The geomechanics classification in rock engineering applications. *Proc 4th Int Congr rock Mech* 41–48
- Bieniawski ZT (1989) *Engineering rock mass classification: a complete manual for engineers and geologists in mining, civil, and petroleum engineering*. John Wiley & Sons, Inc., New York
- Chen Z (1995) Recent developments in slope stability analysis. In: *8th International Congress of Rock Mechanics*. International Society for Rock Mechanics, pp 1041–1048
- Chen C, Pan E, Amadei B (1998) Determination of deformability and tensile strength of anisotropic rock using Brazilian tests. *Int J Rock Mech Min Sci* 35:43–61
- CMRI (1987) *Geomechanical classification of roof rocks vis-à-vis roof supports- S&T project report*. Dhanbad,
- Deere DU, Hendron AJ, Patton FD, Cording EJ (1967) Design of surface and near-surface construction in rock. *8th US Symp. Rock Mech. (USRMS)-Failure Break*. Rock 237–302
- Donath FA (1961) Experimental study of shear failure in anisotropic rocks. *Geol Soc Am Bull* 72:985–990. [https://doi.org/10.1130/0016-7606\(1961\)72\[985:ESOSFI\]2.0.CO;2](https://doi.org/10.1130/0016-7606(1961)72[985:ESOSFI]2.0.CO;2)
- Donath FA (1964) Strength variation and deformational behavior in anisotropic rock. In: Judd W (ed) *State of Stress in the Earth's Crust*. New York, pp 281–298
- Garagon M, Çan T (2010) Predicting the strength anisotropy in uniaxial compression of some laminated sandstones using multivariate regression analysis. *Mater Struct* 43(4):509–517
- Gonzalez de Vallejo LI (1983) A new rock classification system for underground assessment using surface data. In: *International Symposium on Engineering Geology and Underground Construction*. Lisbon, pp 85–94
- Gonzalez de Vallejo LI (1985) Tunnelling evaluation using the surface rock mass classification system SRC. In: *ISMR Symposium on the Role of Rock Mechanics in Excavations for Mining and Civil Works*. Zacatecas, Mexico, pp 458–466
- Gonzalez de Vallejo LI (2003) SRC rock mass classification of tunnels under high tectonic stress excavated in weak rocks. *Eng Geol* 69: 273–285. [https://doi.org/10.1016/S0013-7952\(02\)00286-7](https://doi.org/10.1016/S0013-7952(02)00286-7)
- González NA, Vargas PE, Carol I et al (2016) Comparison of discrete and equivalent continuum approaches to simulate the mechanical behavior of jointed rock masses. In: Wuttke, Bauer, Sánchez (eds) *1st International Conference on Energy Geotechnics*. Taylor & Francis Group, London, pp 255–262
- Heng S, Guo Y, Yang C et al (2015) Experimental and theoretical study of the anisotropic properties of shale. *Int J Rock Mech Min Sci* 74: 58–68. <https://doi.org/10.1016/j.ijrmm.2015.01.003>
- Hoek E (1994) Strength of rock and rock masses. *ISRM News J* 2:4–16

- Hoek E, Brown ET (1988) The Hoek-Brown failure criterion - a 1988 update. In: 15th Canadian Rock Mechanics Symposium. pp 31–38
- Hoek E, Kaiser PK, Bawden WF (1995) Support of underground excavations in hard rock. Balkema, Rotterdam
- Hoek E, Carranza-torres C, Corkum B (2002) Hoek-brown failure criterion – 2002 edition. In: Proceedings of NARMS-Tac. pp 267–273
- Hoek E, Marinos PG, Marinos VP (2005) Characterisation and engineering properties of tectonically undisturbed but lithologically varied sedimentary rock masses. *Int J Rock Mech Min Sci* 42(2):277–285
- Huan J, He M, Zhang Z, Li N (2019) Parametric study of integrity on the mechanical properties of transversely isotropic rock mass using DEM. *Bull Eng Geol Environ* 79:2005–2020
- Hudson J, Harrison J (2000) Engineering rock mechanics: an introduction to the principles, 2nd edn. Elsevier Science Ltd, Oxford
- IWPCO (2004) Karun IV dam and hydropower plant- report on increasing the length of grouting galleries of left abutment. Tehran
- IWPCO (2007) Engineering geology report of Rudbar-e-Lorestan dam and hydropower plant. Tehran
- IWPCO (2010) Khersan III dam and hydropower plant- final report of diversion tunnel. Tehran
- Jaeger JC (1960) Shear failure of anisotropic rocks. *Geol Mag* 97:65–72
- Jaeger JC, Cook NG (1979) Fundamentals of rock mechanics. Methuen, London
- Jakubec J, Laubscher DH (2000) The MRMR rock mass rating classification system in mining practice. In: MassMin 2000. Brisbane, pp 413–421
- Javadi M, Sharifzadeh M, Shahriar K (2010) A new geometrical model for non-linear fluid flow through rough fractures. *J Hydrol* 389:18–30. <https://doi.org/10.1016/j.jhydrol.2010.05.010>
- Khatik VM, Nandi AK (2018) A generic method for rock mass classification. *J Rock Mech Geotech Eng* 10:102–116. <https://doi.org/10.1016/j.jrmge.2017.09.007>
- KRWA (2016) Kerman water conveyance tunnel- final report of engineering geology. Kerman
- Laubscher DH (1990) A geomechanics classification system for the rating of rock mass in mine design. *J South Afr Inst Min Metall* 90: 257–273. [https://doi.org/10.1016/0148-9062\(91\)90830-F](https://doi.org/10.1016/0148-9062(91)90830-F)
- Lauffer H (1958) Gebirgsklassifizierung für den stollenbau. *Geol und Bauwes* 24:46–51
- Lin H, Cao P, Wang Y (2013) Numerical simulation of a layered rock under triaxial compression. *Int J Rock Mech Min Sci* 60:12–18. <https://doi.org/10.1016/j.ijmms.2012.12.027>
- Lowson AR, Bieniawski ZT (2013) Critical assessment of RMR based tunnel design practices: a practical engineer's approach. In: Proceedings of the SME: Rapid Excavation & Tunneling Conference. Washington, pp 23–26
- Maazallahi V, Majdi A (2020) 3D Characterization of uniaxial compressive strength of transversely-isotropic intact rocks. *J Min Environ* 11:629–641. <https://doi.org/10.22044/jme.2020.9039.1791>
- Majdi A, Hassani F (1989) Access tunnel convergence prediction in longwall coal mining. *Int J Min Geol Eng* 7:283–300. <https://doi.org/10.1007/BF00896593>
- Marinos P, Hoek E (2001) Estimating the geotechnical properties of heterogeneous rock masses such as Flysch. *Bull Eng Geol Environ* 60:85–92
- Marinos PV (2010) New proposed GSI classification charts for weak and complex rock masses. In: 12th Bulletin of the Geological Society of Greece International Congress. Patras, pp 1248–1258
- Öge IF (2017) Assessing rock mass permeability using discontinuity properties. *Procedia Eng* 191:638–645. <https://doi.org/10.1016/j.proeng.2017.05.373>
- Pacher F, Rabcewicz L, Golser J (1974) Zum derzeitigen stand der gebirgsklassifizierung im stollen- und tunnelbau. In: 22. Geomechanik-Kolloquium. Salzburg
- Palmström A (1995) RMI- a rock mass characterization system for rock engineering purposes, PhD Thesis, University of Oslo. University of Oslo
- Pells PJ, Bieniawski ZT, Hencher SR, Pells SE (2017) Rock quality designation (RQD): time to rest in peace. *Can Geotech J* 54:825–834. <https://doi.org/10.1139/cgj-2016-0012>
- Ramamurthy T (1993) Strength and modulus responses of anisotropic rocks. In: Brown ET (ed) Comprehensive rock engineering. Pergamon press, pp 313–329
- Ramamurthy T (1996) Stability of rock mass. *Indian Geotech J* 16:1–73
- Ritter W (1879) Die statik der tunnelgewölbe. Springer, Berlin
- Romana M (1985) New adjustment ratings for application of Bieniawski classification to slopes. In: International symposium on the role of rock mechanics. Zacatecas, Mexico, pp 49–53
- Saeidi O, Rasouli V, Geranmayeh Vaneghi R, Gholami R (2014) A modified failure criterion for transversely isotropic rocks. *Geosci Front* 5:215–225. <https://doi.org/10.1016/j.gsf.2013.05.005>
- Saroglou H, Tsiambaos G (2008) A modified Hoek-Brown failure criterion for anisotropic intact rock. *Int J Rock Mech Min Sci* 45:223–234. <https://doi.org/10.1016/j.ijmms.2007.05.004>
- Saroglou C, Qi S, Guo S, Wu F (2018) ARMOR, a new classification system for the rating of anisotropic rock masses. *Bull Eng Geol Environ*, vol 78, pp 3611–3626
- Sen Z, Sadagah BH (2003) Modified rock mass classification system by continuous rating. *Eng Geol* 67:269–280
- Senior LA, Goode DJ (1999) Ground-water system, estimation of aquifer hydraulic properties, and effects of pumping on ground-water flow in Triassic sedimentary rocks in and near Lansdale, Pennsylvania, No. 99-422. US Dept. of the Interior, US Geological Survey
- Sheorey PR (1997) Empirical rock failure criteria. Balkema, Rotterdam
- Singh B, Goel RK (1999) Rock mass classification: a practical approach in civil engineering. Elsevier, Amsterdam
- Singh VK, Singh D, Singh TN (2001) Prediction of strength properties of some schistose rocks from petrographic properties using artificial neural networks. *International J Rock Mech Min Sci* 38(2):269–284
- STP Consulting Engineers (2018) Report on geology and engineering geology of Kaniguizhan dam site. Tehran,
- Terzaghi K (1946) Rock defects and loads on tunnel supports. *Rock Tunn with steel Support* 17–99
- Tomas R, Delgado J, Seron JB (2007) Modification of slope mass rating (SMR) by continuous functions. *Int J Rock Mech Min Sci* 44:1062–1069. <https://doi.org/10.1016/j.ijmms.2007.02.004>
- Tziallas GP, Saroglou H, Tsiambaos G (2013) Determination of mechanical properties of flysch using laboratory methods. *Eng Geol* 166: 81–89
- Venkateswarlu V, Ghose AK, Raju NM (1989) Rock-mass classification for design of roof supports - a statistical evaluation of parameters. *Min Sci Technol* 8:97–107. [https://doi.org/10.1016/S0167-9031\(89\)90507-0](https://doi.org/10.1016/S0167-9031(89)90507-0)
- Wickham GE, Tiedemann HR, Skinner EH (1972) Support determinations based on geologic predictions. In: Proc. 1st North American Rapid Excavation & Tunneling Conference (RETC). pp 43–64
- Wittke W (2014) Rock mechanics based on an anisotropic jointed rock model (AJRM). Wiley Blackwell, Berlin
- Wu Q, Kulatilake PHSW (2012) REV and its properties on fracture system and mechanical properties, and an orthotropic constitutive model for a jointed rock mass in a dam site in China. *Comput Geotech* 43:124–142. <https://doi.org/10.1016/j.compgeo.2012.02.010>
- Zhang L (2016) Determination and applications of rock quality designation (RQD). *J Rock Mech Geotech Eng* 8:389–397. <https://doi.org/10.1016/j.jrmge.2015.11.008>
- Zhang L (2017) Engineering properties of rocks, 2nd edn. Elsevier Ltd.